TAMPERE UNIVERSITY OF TECHNOLOGY

JESSE ASIKAINEN

ISLANDING OF A FULL POWER CONVERTER GRID INTERFACE

Master of Sciense Thesis

Examiner: Professor Sami Repo
Thesis examiner and subject were approved in the Faculty of Computing and Electrical Engineering council meeting on 08th June 2011

TIIVISTELMÄ

TAMPEREEN TEKNILLINEN YLIOPISTO
Sähkötekniikan koulutusohjelma
ASIKAINEN, JESSE: Saareketilanteet täystehokonvertterilla
Diplomityö, 63 sivua, 1 liitesivu
Tammikuu 2012
Pääaine: Sähköenergiatekniikka
Tarkastaja: Professori Sami Repo
Avainsanat: saarekkeet, saarekkeen tunnistaminen, hajautettu tuotanto, täystehokonvertteri

Osa älykkäiden sähköverkkojen ideologiaa on uusi lähestymistapa sähköverkon saareketilanteisiin. Älykkäät sähköverkot ja hajautettu tuotanto voivat tulevaisuudessa mahdollistaa esimerkiksi tehon syötön jakeluverkosta kantaverkkoon ja jakeluverkon yksittäisen lähdön operoinnin itsenäisenä järjestelmänä. Näissä tilanteissa sähköverkon suojaukselle ja säädölle asetetaan uudenlaisia vaatimuksia kuten saarekkeen tunnistaminen ja hajautetun tuotannon kyky pitää yllä verkon jännitettä ja taajuutta. Täystehokonvertteri on uuden hajautetun tuotannon yleisin verkkoon liittämiskeino ja mahdollistaa suojausfunktioiden ja verkon ylläpitämisen implementointia hajautetun tuotannon yksiköihin.

Tässä diplomityössä tutkitaan saarekkeen muodostumista sekä siihen liittyviä ilmiöitä kuten turvallisuusnäkökohtia ja mahdollisia hyötyjä. Kirjallisuudessa esiteltyjä saarekkeen tunnistusmenetelmiä sekä niiden hyviä ja huonoja puolia käydään läpi. Saarekkeen muodostumista tutkitaan käytännön testien avulla ja taajuuden poikkeuttamiseen reaktiivisen virran avulla perustuvan saarekkeen esto menetelmän osalta. Saarekkeen tunnistusmenetelmien testaukseen ja käyttöön liittyviä verkko vaatimuksia hyödynnetään testauksessa ja tuloksia tarkastellaan standardoinnin pohjalta.

Tuloksista selviää saarekkeen taajuuden ja jännitteen käyttäytyminen erilaisilla pätö – ja loisteho tasapainoilla sekä verkko invertterin käyttäytyminen ilman saarekkeen tunnistusmenetelmää ja sen kanssa. Tuloksien perusteella voidaan arvioida saarekkeen tunnistusmenetelmän toimivuutta ja soveltuvuutta erilaisiin verkko vaatimuksiin ja ympäristöihin. Verkko invertterin toiminta ilman saarekkeen esto menetelmää todennetaan ja olemassa olevien tuotteiden osalta voidaan arvioida saarekkeeseen joutumisen mahdollisuutta ja todennäköisyyttä.

ABSTRACT

TAMPERE UNIVERSITY OF TECHNOLOGY
Master's Degree Programme in Electrical Engineering
ASIKAINEN, JESSE: Islanding of a full power converter grid interface
Master of Science Thesis, 63 pages, 1 Appendix page
January 2012
Major: Power engineering
Examiner: Professor Sami Repo
Keywords: islanding, islanding detection, anti-islanding, distributed generation full power converter

A part of smart grid ideology is a new approach to islanding of power system. Smart grids and distributed generation can e.g. enable power flow upstream from distribution network and operation of distribution branch as an individual power system. These scenarios introduce new requirements for protection and control of the power system such as detection of islanding and the ability of distributed generation to maintain voltage and frequency of the power system. Full power converter is the most used way of connecting new distributed generation to power system and it enables implementation of protection functions and grid controlling abilities into distributed generation units.

This thesis studies islanding of power systems and related phenomena such as safety aspects and possible benefits of islanding. Islanding detection methods presented in literature and their benefits and downsides are reviewed. Islanding and an anti-islanding method based on frequency diverging by reactive current injection are studied also from practical perspective by a miniature demonstration. Grid codes and standardization related to islanding are utilized in testing and results are studied on the grounds of standardization.

Results show the frequency and voltage behavior of the islanded system with different reactive – and active power balances and behavior of the grid interface inverter with and without islanding prevention functionality. On basis of these results the functionality and applicability of this islanding detection method into different environments and compatibility with different grid codes can be evaluated. Functionality of the grid inverter without anti-islanding functionality is verified and as for currently existing products the possibility and probability of unintentional islanding can be assessed.

ALKUSANAT

Tämä diplomityö on kirjoitettu The Switch Drive Systems Oy:n Vaasan yksikössä ja soveltavan osuuden testit on tehty yhtiön Lappeenrannan yksikössä. Työ on osa teknologian ja innovaatioiden kehittämiskeskuksen smart grids and energy markets -projetia. Työn ohjaajana toimi diplomi-insinööri Mikko Pääkkönen ja tarkastajana professori Sami Repo Tampereen teknillisen yliopiston sähköenergiatekniikan laitokselta.

Haluan kiittää The Switch Drive Systemsin Lasse Kankaista erittäin mielenkiintoisesta aiheesta diplomityölle sekä avusta ja neuvoista projektin edetessä. Kiitokset myös työn ohjaajalle ja tarkastajalle, esimiehelleni Jyrki Sorilalle mahdollisuudesta tämän työn tekemiseen ja kollegoilleni tuesta projektin eri vaiheissa. Kiitos myös vanhemmilleni tuesta koko 20-vuotisen koulu-urani aikana.

Vaasassa 2.2.2012

Jesse Asikainen

TABLE OF CONTENTS

ABREVIATIONS AND NOTATION

A	A bold capitol letter stands for a matrix
B	Vector base
$b_{1,2,3}$	A vector
C	Capacitance
$\mathbb{C}$	Group of complex numbers
cf	Chopping fraction
$e_{a0,b0,c0}$	Grid phase voltages
$e_{q,d}$	Grid voltage synchronous components
f	Frequency
E	Expectation value
F	A function
G	Frequency over power charactristic
H	Inertia constant
h	Running number
$i_{1a,1b,1c}$	Instantaneous current fundamental components
$i_{q,d}$	Synchronous current components
i_{ref}	Current reference
j	Imaginary unit
$k_{P,Q}$	Droop slope
K	Controller gain
k	kilo, 10^3
L	Inductance
M	Mega, 10^6
m	Milli, 10^{-3}
n	Running number
P	Real power
Q	Reactive power
R	Resistance
t	Time
T	Period length, transpose
U	Voltage
U_{DC}	DC voltage
U_{DC-Ref}	DC voltage reference
U_h	hth harmonic voltage component
U_{LL}	Phase-to-phase voltage
U_{Neg}	Negative sequence voltage
U_{ph}	Phase voltage
$U_{ph\,Nom}$	Nominal phase voltage
U_{Pos}	Positive sequence voltage

$u_{x,y,z}$	Orthogonal coordinates
u_s	Space vector
U_{UB}	Voltage unbalance
$U_{\alpha,\beta}$	Orthogonal coordinates
U_0	Homopolar coordinate
U_1	Fundamental voltage component
$\hat{V}$	A letter with a circumflex refers to a vector
V	Inverter output voltage
V_{nl}	Inverter idle voltage
$v_{a0,b0,c0}$	Inverter pole voltages
$v_{q,d}$	Synchronous pole voltage components
Q_f	Quality factor
X	Reactance
Y	A three phase connection
Z	Impedance
Γ	Error variable
Δ	Variation interval, a three-phase connection
η	Accuracy
Θ	An angle
Σ	Sum operator
μ	Micro, 10^{-6}
π	A mathematical constant
φ	An angle
$\bar{\Lambda}$	A fourier vector
ω	Angular frequency

AFD	Active frequency drift
AFE	Active front end, a 4-quadrant inverter
AFDPF	Active frequency drift with positive feedback
AFDPCF	Active frequency drift with pulsating chopping fraction
APS	Automatic phase shift
ALPS	Adaptive logic phase shift
ARPS	Adaptive reactive power shift
BR	A breaker
DC	Direct current component of a signal is defined as an average value of that signal
DFT	Discrete Fourier transform, a method for separating frequency components from a sampled signal
DG	Distributed generation, units rated from 0 to 5MW located in distribution branches of the network

DSP	Digital signal processing is used by microprocessors to process discrete signals
ENTSO-E	A harmonized European grid code
FPC	Full power converter, a frequency conversion unit rated to nominal power of a production unit
FRT	Fault ride through refers to power system equipment's ability to stay operational during a grid fault
IEEE	Institute of electrical and electronics engineers
IEC	International electrotechnical commission
IGBT	Isolated-gate bipolar transistor is an electronic component utilized by modern power electronic devices
NDZ	Non detection zone is a performance index for islanding detection methods
PCC	Point of common coupling is the point in which for example a distributed generation unit connects to power grid
PF	Power factor
PID	Proportional, integral, derivative, -controller
PLL	Phase locked loop is a servo system which is used to make one signal track another signal
PQ-control	A control scheme in which converter unit is operated as a current source
PWM	Pulse width modulation is the most widely used method of controlling inverter output voltage
RMS	Root mean square value defines an equal dc level for a sinusoidal signal
SAIDI	System average interruption duration index is an index describing average interruption duration in power system
SAIFI	System average interruption frequency index is an index describing interruption frequency of a power system
SFS	Sandia frequency shift is an active islanding detection method based on frequency deviation
SVS	Sandia voltage shift is an active islanding detection method based on voltage amplitude deviation
SVPWM	Space vector pulse width modulation
THD	Total harmonic distortion is the amount of harmonic content in a signal
VSI-control	A control scheme in which converter unit is operated as a voltage source

1 INTRODUCTION

Smart grids are a modern tendency of power grids. One part of smart grid ideology is distributed generation which is sited within the distribution network. Originally distribution network has not been designed to deliver power upstream to the grid which surfaces new kind of design issues related to protection and control of the power system. Distributed generation often utilizes renewable energy sources such as wind – and solar power and electrical energy is converted to a suitable form to be fed to AC network with utilization of power electronics. Modern power electronics devices are controlled with micro controllers which make it possible to implement also protection and grid control features into distributed generation units. This is motivated by the fact that protection relays dedicated to e.g. islanding detection are expensive in comparison to price of a small distributed generation unit.

Islanding is a situation in which a section of distributed network becomes disconnected from the main power system as a result of fault or some planned event. If this section comprises generation it is a concern of safety for both humans and equipment. The biggest concern for personnel is the risk of power system remaining energized while there is an assumption that the system is dead or any protection failing because of distributed generation feeding the network. For power system equipment islanding may result in various kinds of over voltages and over currents leading to damage the equipment. Intentional islanding also offers a possibility to increase power quality by feeding some section of the power system which could not be fed otherwise due to fault or planned power break. Control methods for a modern power inverter offer various possibilities to monitor and affect electrical quantities which can be used to detect islanding of the power system.

Islanding detection methods can be categorized broadly in local – and remote techniques. Remote techniques are based on communication of the distributed generation and power system. This thesis concentrates on local techniques which can be further divided into passive –, active – and hybrid techniques.

Passive islanding detection operates on the measurable electrical quantities at the point where the distributed generation unit is connected to the network. From these quantities different variables such as voltage and frequency are monitored in order to detect islanding situations. The shortcoming of passive islanding detection methods is that they are not very effective. Positive side of passive methods is that they do not affect power quality. Currently passive methods such as frequency and voltage monitoring are most referred in standardization and most used in all power generation. Also more sophisticated passive methods such as voltage unbalance -, harmonic content - and

phase monitoring have been developed in order to increase the sensitivity of passive methods.

Active islanding detection methods operate on the principle of introducing disturbances on some electrical derivative and monitoring the effect of those disturbances. Some active methods are referred to as very effective but the shortcoming is that they affect power quality negatively. Many active methods are mathematically complex and require vast amount of computing capacity, thus excluding their implementation in regular inverter control unit without additive devices. In some countries grid codes restrict using of some active methods directly. E.g. in Germany an impedance measurement based method is required for micro production but in Great Britain this method is forbidden. Grid codes introduce restrictions in using of active detection methods also indirectly in power quality requirements.

Hybrid techniques are combinations of passive and active methods with the objective to combine good qualities of both. I.e. unaffected power quality during normal operation and effective islanding detection.

As islanding is a quite new issue for inverter manufacturers and distributed generation operators, also standardization for testing of islanding detection methods and regulations concerning islanding has been done very recently or is still ongoing. In this thesis designing and building of a test setup for islanding, as well as testing of islanding and anti-islanding method based on reactive power variation is conducted. Principles for test environment and procedure are adapted from IEEE 1547.1 but also European standardization is referred. Objective is to gather information on islanding and on usability and performance of the anti-islanding method available. Islanding test setup is build with 12A inverters and a parallel RLC load is introduced as a stabilizing element in the islanded system. Testing is done with matched PQ-balance within the island and with load inductance diverged in one percent steps within a range of +/-5%. Results are investigated from the perspective of frequency and voltages of the islanded system and behavior of the grid interface inverter is outlined.

This thesis constitutes of literature survey in chapters two and three and applied section in chapter four. In chapter two the phenomenon of islanding and risks and benefits related to islanding are studied. Also principles of inverter control methods are discussed. In chapter three passive, active and hybrid islanding detection methods and their applicability are investigated. Chapter four focuses on practical side of islanding phenomenon in designing of the test setup, regulations and standardization concerning islanding and actual testing of islanding and investigation of test results is carried out. Chapter five handles summary and conclusions of islanding and islanding detection as well as discusses the future interests in testing and development of islanding functionality.

2 ISLANDING AND A FULL POWER CONVERTER

Islanding is a situation in which a minor part of the power system is operating independently of the rest of the power system. This is due to distributed generation units remaining operational when connection to the main grid is lost. DG stands for distributed generation which consists of small power units connected to distribution branches of the network ranging from 0 to 5MW in power. This chapter focuses on effects of a full power converter grid interfaced DG on power system and control principles of the grid interface.

Islanding relates to issues concerning safety, damage to equipment connected to the network and power quality issues. Thus, formation of an unintentional island is a concern for utility companies. [1] Intentional islanding can also be used to improve power quality. [2, p. 1; 4]

2.1 Effects of islanding and DG on power grid

Improving reliability and availability of electricity networks is gaining more attention year by year. Intentional islanding of networks has been suggested to be one of the solutions to achieve tightening power quality requirements. DG units can be used to restore power supply to the loads during a grid failure in the upstream network and also as a part of power restoration arrangements by backup connections. These measures will reduce the outage time of customers in the islanded part of the network as well as number of customers suffering from outage. [2, p. 1] According to study conducted in [2] by placing DG units in distribution network it is possible to improve network reliability figures. In [3], [4], [5], [6], [7] and [8] the effects of introducing DG into distribution network are discussed. Positive impacts are called “system support benefits” which consist of voltage support and loss reduction, release of transmission capacity and deferments of grid investments [3, p. 1].

2.1.1 Reliability

Problems related to reliable power supply are related to faults occurring in network components. Since distribution networks are traditionally operated radially it follows that a fault in single network component is due to cause outage to a large number of customers. Correctly placed DG units may help to restore power supply to customers before repairing of the fault can be done. Thus, positive effects of DG units on reliability are strongly dependent on placement of the units. [2, p. 1, 4]

Network reliability can be analyzed numerically by means reliability figures which relate to fault frequencies and outage times of the network. In [2] used reliability figures are SAIDI and SAIFI which stand for system average interruption duration index and system average interruption frequency duration index, respectively. In order to improve network reliability improving SAIDI and SAIFI then becomes the main concern but it has to be noted that it is always a technical-economical optimizing task. Also, economical benefits increase when failure frequency and outage costs of the distribution network increase. [2, pp. 1-2]

When comparing influences of intended islanding and traditional methods of improving distribution network reliability such as back-up connections it is found that intended islanding performs well both technically and economically. In [2] it is suggested that solutions can be found in which DG compares better to e.g. building new back-up connections, replacing old back-up connections with DG and replacing low loaded branch, such as a summer cottage, with a DG unit.

2.1.2 Voltage regulation

Traditionally voltage regulation is based on radial power flows from the substation to the loads by use of tapping of transformers and switched capacitors. DG makes traditional approaches impractical by introducing new power flow directions. For example a DG unit placed downstream near a load-tap-changing transformer will cause the voltage regulator to tap down the voltage as it recognizes only power flowing through the transformer. At the end of the distribution branch this may cause voltage to drop out of accepted range. [3, p. 2-4] Introduction of DG is also capable of producing voltage regulation related over voltages into distribution network. This may happen for example when DG unit is connected near the end of the distribution branch and is feeding large amount of power upstream the network. In this situation voltage near the DG unit may rise over acceptable limits. It is important to take voltage regulation issues under consideration when planning implementation of DG. [4, pp. 3-5]

2.1.3 Abnormal over voltages

In addition to voltage regulation related problems which occur during normal operation there is potential other issues to be considered with DG such as ground fault over voltages and resonant over voltages which both specifically relate to islanding of a power system. Ground faults can generate over voltages into distribution network when one phase of a three-phase four-wire system is faulted to the neutral. Once this is happened the substation circuit breaker will open and DG remains feeding the system. This results in that both unfaulted phases will be subjected to voltages as high as 191 percent of nominal if the system is operating with 10 percent over voltage in prior to fault as equation (1), where U_{ph} and $U_{ph\,Nom}$ stand for during fault and nominal phase voltages, shows.

$$U_{ph} = \sqrt{3}\, U_{ph\,Nom} \cdot 1{,}1 = 1{,}91\, U_{ph\,Nom} \quad (1)$$

Voltages this high present themselves mainly after opening of the substation breaker since the grounding voltages will be held down by grounding bank effect of substation transformer prior to islanding of the system. In [4] it is suggested to use effective grounding of substation transformer, ground fault overvoltage protection and transfer trip relaying of the DG unit as a solution to ground fault over voltages. [4, pp. 1-3]

2.1.4 Resonant over voltages

Islanding of a DG system affects also the impedances of the system and thus introduces a possibility for resonant over voltages. This type of over voltages can represent themselves under faulted or unfaulted operating conditions and severity of them depends on damping of the system. Damping factor of the system is in relation to loads connected to the network and thus biggest over voltages occur under light loading conditions. [4, pp. 3-4]

Another type of resonant overvoltage with a system containing DG is ferroresonance. It is an interaction between non-linear magnetizing reactance of transformer and system capacitance. Ferroresonance may lead to over voltages as high as 3 to 4 per unit. It is mainly an issue with ungrounded DG interfaces but may present itself to some extend with all grid interfaces. In order for ferroresonance to occur the system must be operating in islanded mode, there has to be an oversupply of power, island has to have sufficient capacitance and a transformer acting as a non-linear reactance. [4, pp. 3-4]

2.1.5 Voltage Flicker

Voltage flicker is visible variation in lighting loads of the network caused by sudden changes in voltage level [5, p. 1]. Distributed generation may cause voltage flicker on feeders where it is present. Flicker is related to connection events, i.e. starting and stopping of DG units, and step changes in DG output. With wind – and solar energy fluctuations in power level are common as power level changes with primary energy source intensity. It is calculated that a one meter change in wind-speed results in 20% fluctuations in power level when operating near rated power. Also tower shadow effect and bandwidth limitations of pitch system can cause flicker. With a three bladed turbine the output power can be seen to drop three times per revolution due to tower shadow effect. In pitch-controlled turbines limitations in bandwidth of the pitch mechanism cause fluctuations in power level especially when operating near rated power because of over speed situations. [5, pp. 2-5]

Calculation of a single turbine flicker emission is rather complicated and an analytical method for determining short term flicker from a set of arbitrarily chosen voltage disturbances doesn’t exist. It is recommended in IEC-61400-21 that flicker emission from a single turbine should be determined by measurements. Measurements should be based on voltage and current because measurements based only on voltage could be disturbed by the background flicker in the grid. [5, p. 5]

2.1.6 Losses

Introduction of DG will always have an impact on losses of a distribution network. A DG unit with a full power converter operated grid interface can also compensate reactive power within a distribution branch. It has to be taken into account when designing a power converter to have more current capacity than nominal real power of the primary energy source of the unit. This is to maintain capability to inject reactive current also when operating with nominal real power. A DG unit with a 10-20% output capacity of the feeder demand can have a significant effect on reducing losses. On the other hand large DG units such as wind turbines will almost always require reinforcements of the distribution network or a separate connection to the main grid. [3, pp. 3-4]

2.1.7 Harmonics

Harmonics produced by a modern full power converter are a consequence of switching events of IGBTs. IGBT is an abbreviation from isolated-gate bipolar transistor which is an electronic component used in most modern power electronics applications related to DG. Harmonic current components are not desired in a power system since they consume current capacity and cause heating and overloading of the equipment. THD or total harmonic distortion is calculated with equation (2).

$$\mathrm{THD} = \frac{\sqrt{\sum_{h=2}^{n} U_h^2}}{U_1} \tag{2}$$

In (2) U_1 is the root-mean-square, or RMS-value, of the fundamental voltage component and U_h is the RMS-value of the *h*th harmonic. According to IEEE standardization first 50 harmonics are used when calculating THD. Since harmonic content clusters around switching frequency it is evident that increasing the switching frequency causes the harmonic content to be of a higher order. With bus-clamped switching methods harmonic content clusters around half of the switching frequency in addition to switching frequency. When comparing different switching methods it is noted in [6] that bus-clamped switching schemes produce significantly higher amount of harmonic content than conventional sinusoidal pulse width modulation. [6, pp. 3-5]

2.1.8 Automatic reclosing

A common problem related to distribution networks with DG is failing of automatic reclosing. When a safety relay of a feeder detects a fault and executes an automatic reclosing operation in order to clear the fault and DG unit remains operational during dead time of the feeder it is likely to remain feeding fault current into the fault and thus cause the reclosing to fail. This may happen with short circuit faults but especially it is problematic with ground faults since ground fault currents are small and DG unit might not provide a ground current source. In addition to failing of the reclosing it is a safety issue when a feeder remains energized during dead time of the reclosing which can present

itself as dangerous voltages to ground. This makes it highly important to disconnect DG unit from the grid during dead time of the automatic reclosing. [7; 8, pp 1-2]

In most cases re-coordination of the protection needs to be considered when DG is installed into grid. For example dead time of automatic reclosing might have to be lengthened or with some relays reclosing can be blocked if the downstream grid is energized. Reclosing of the feeder may also cause damage to DG unit if it is connected to grid during recovery voltage. In case of grid connected rotating machines out-of-phase reclosure is highly potential to cause damage to generator equipment but full power converter operated DG unit typically is capable of protecting itself during out-of-phase reclosing. [8, p. 2]

2.2 Control principles of a full power converter

In a conventional power system synchronized generators are responsible for voltage and frequency control of the grid. Within micro grids it is common that generation units are not synchronous generators but grid interface is realized with a power electronic converter. Commonly this is due to characteristics of the primary energy source and to achieve better efficiency. Therefore, control methods of grid interface inverters are crucially important when planning islanded operation of a power system. [9, p. 1]

When grid is connected DG units are operating in PQ control mode. I.e. units are controlling their real - and reactive power according to given set point whereas output voltage and frequency are determined by the grid. When switched to island mode operation unit needs to control its output voltage and frequency whereas power is determined by consumption present within the island. This is referred to as U-f control mode, or inverter operating as a voltage source. Thus, it becomes evident that switching between these control schemes is vital for a DG unit to remain operational during transition from grid connected operation to islanded operation and vice versa. [9, p. 3] This thesis concentrates on a single converter operation but it is noted in [9] that introduction of more parallel units presents a similar but more complex problem of switching control schemes.

2.2.1 Modulation strategies

Modulation strategies are methods for controlling states of the power electronic switches. Most power electronic applications utilize switch mode of the switches since this minimizes the commutation losses of the switches when compared to operation in linear region. [10]

In figure 2.1 principle of the topology of a grid interface inverter is presented. Six-step modulation is an early modulation technique to control three-phase inverter which uses a sequence of six switching patterns to generate a full cycle of three phase voltages. The inverter has eight states defined by states, merely on or off, of six switches. All three inverter legs have two switches as in figure 2.1. In addition to six active stages inverter has two passive stages in which all three lower or upper switches of the legs are

on. Today six-step modulation is very unlikely to be used in new designs because of very high harmonic content of the output voltage but it is often used to illustrate a three-phase inverter operation simply. Inductances at the inverter output filter the output current to be sinusoidal. [10]

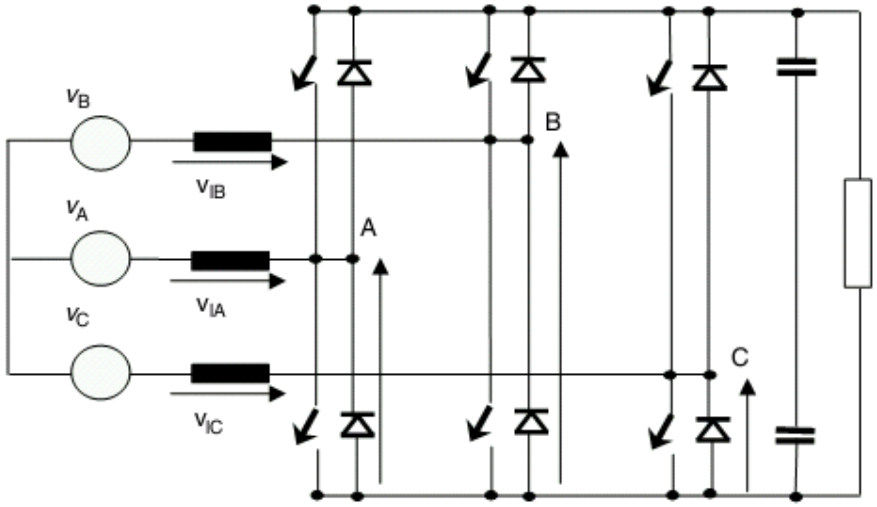

Figure 2.1. *Basic topology of a six-switch grid interface inverter. [11, p. 307]*

2.2.2 Pulse width modulation

In most modern power electronics devices pulse width modulation, or PWM, is adapted as a method for control. The basic idea behind PWM techniques is that the load sees an average value of voltage which is formed by switching a constant dc voltage on and off with varying duty cycle. With utilization of high switching frequency and suitable LC filtering the output current of the inverter does not follow individual switching events and it is sinusoidal. [10]

There are several different methods for generating periodic rectangular waveforms with varying duty cycle from which one of the most adapted is the carrier-based PWM technique. In carrier based PWM technique a control signal is compared with triangular waveform. Control signal is the fundamental waveform of desired inverter output voltage and triangular wave has the frequency defined as the switching frequency of the inverter. Switching frequency is determined on basis of heat absorption capabilities of switches, efficiency and desired harmonic content. [10]

2.2.3 Space-vector modulation

Modern pulse width modulation strategies today are called space-vector pulse width modulation, SVPWM, respectively. Compared to conventional PWM strategies it offers improved dc voltage utilization and less commutation losses. [11, p. 119]

The core idea of vector transformation from coordinates $u_x(t)$, $u_y(t)$ and $u_z(t)$ to coordinates $u_d(t)$, $u_q(t)$ and $u_0(t)$ is presented in [10]. It is based on equations (3) and (4) where $a = e^{j\left(\frac{2\pi}{3}\right)}$.

$$u_s = \frac{2}{3}[u_x(t) + au_y(t) + a^2u_z(t)] \tag{3}$$

$$\vec{V} = b_1(\omega_j)u_d + b_2(\omega_j)u_q + b_3(\omega_j)u_0 \tag{4}$$

Equation (3) states that a three-phase system defined by u_x, u_y and u_z can be represented by a rotating vector u_s in complex plane. (4) is a representation showing that a base in a vector space consists of a system of vectors $B(b_1, b_2, b_3)$ that is unique representation of any member $\vec{V}$ of that vector space as a linear combination of vectors from B. The operation of transforming three-phase system into a unique vector followed by a transformation from orthogonal coordinates in quasi-DC coordinates is called Park/Clarke transform for three-phase systems. Clarke transform states that any vector in the complex plane can be expressed with two orthogonal coordinates (U_α, U_β) and a homopolar coordinate (U_0) as in equation (5). Park transform transforms these two coordinates (α, β) through a vector rotation with the rotational frequency of the electrical system. Park transform, presented in (6), is not necessary for the presentation of SVPWM algorithms but it is most often used in professional discourse. These two transforms may also be expressed together and they have an inverse which allows transformation back to phase measures. [11, pp.116-117]

$$\begin{bmatrix} U_\alpha \\ U_\beta \\ U_0 \end{bmatrix} = \begin{bmatrix} 1 & -\frac{1}{2} & -\frac{1}{2} \\ 0 & \frac{\sqrt{3}}{2} & -\frac{\sqrt{3}}{2} \\ \frac{1}{2} & \frac{1}{2} & \frac{1}{2} \end{bmatrix} = \begin{bmatrix} U_x \\ U_y \\ U_z \end{bmatrix} \tag{5}$$

$$\begin{bmatrix} U_d \\ U_q \\ U_0 \end{bmatrix} = \begin{bmatrix} \cos\theta & \sin\theta & 0 \\ -\sin\theta & \cos\theta & 0 \\ 0 & 0 & 1 \end{bmatrix} = \begin{bmatrix} U_\alpha \\ U_\beta \\ U_0 \end{bmatrix} \tag{6}$$

The advantage of vectorial methods and operating in d-q frame is that they provide high performance current control and the possibility to control active and reactive power references separately. To develop a mathematical model for a grid interface inverter presented in figure 2.1 phase voltages can be defined as in equation (7).

$$\begin{aligned} e_{a0} &= R_r i_{1a} + L_r \frac{di_{1a}}{dt} + v_{a0} \\ e_{b0} &= R_r i_{1b} + L_r \frac{di_{1b}}{dt} + v_{b0} \\ e_{c0} &= R_r i_{1c} + L_r \frac{di_{1c}}{dt} + v_{c0} \end{aligned} \tag{7}$$

With vectorial methods discussed in last paragraph input voltages can be transformed into synchronous reference frame which yields to equation (8).

$$\begin{aligned} e_d &= R_r i_d + v_d + L_r \frac{di_d}{dt} - \omega L_r i_q \\ e_q &= R_r i_q + v_q + L_r \frac{di_q}{dt} - \omega L_r i_d \end{aligned} \tag{8}$$

In (8) grid current is decomposed into two components from which i_q stands for active current and i_d stands for reactive current. With i_d current reference the power factor of the converter can be controlled. Current reference for i_q is usually provided by the dc voltage controller when inverter is in normal, grid-connected, operation. [11, pp. 308-309]

2.2.4 PQ inverter control

An inverter connected to the main grid and operating in PQ control injects real power to grid as it is available at its dc input. Amount of reactive power is determined on basis of locally or centrally predetermined set point. Determination of current references is illustrated in figure 2.2. [9, p. 3]

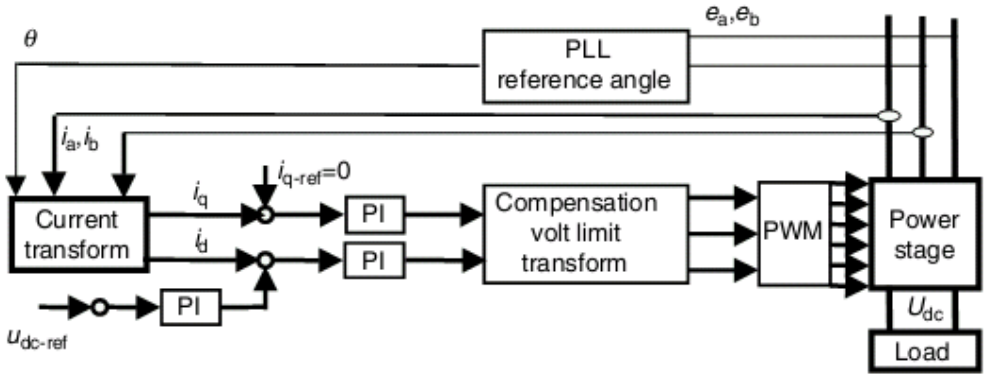

Figure 2.2. *Basic control structure for inverter active – and reactive currents in PQ control mode. [11, p. 309]*

Control of active current is based on dc voltage level error which is the difference between actual dc voltage and preset value of dc voltage, U_{dc} and U_{dc-ref} respectively. DC voltage controller is of PI-type and provides an active current reference as an output. DC voltage controller is also referred to as outer loop of the current controller. By use of i_q current reference and measured value of active current, modulation index is determined. Modulation index determines the voltage at the inverter output and thus controls the active current flowing into or from the grid. Modulation index is determined by active current controller, or inner loop of active current controller, which is also of PI-type. [9, p.3; 12, pp. 4-7]

Reactive current control is realized also with a PI-type controller. Reactive current control relates closely to phase synchronization of the grid interface inverter. Synchronization to phase voltages can be achieved with phase locked loop, i.e. PLL, structure or by utilization of PI and PD type controllers. PLL is a servo system which consists of phase detector, low-pass filter and voltage controlled oscillator. Basic PLL structure is presented in figure 2.3. Basic idea behind the structure is that it will cause one signal to track another one, thus in case of a power converter it will keep the output frequency of the inverter synchronized with the grid in frequency as well as in phase. It is shown in [13] that signal of the voltage oscillator is in quadrature with input signal when the fre-

quency difference between grid and power inverter output becomes zero. Reactive power fed or taken from grid is controlled with i_d current reference. [12, p. 10; 13, pp. 1-2]

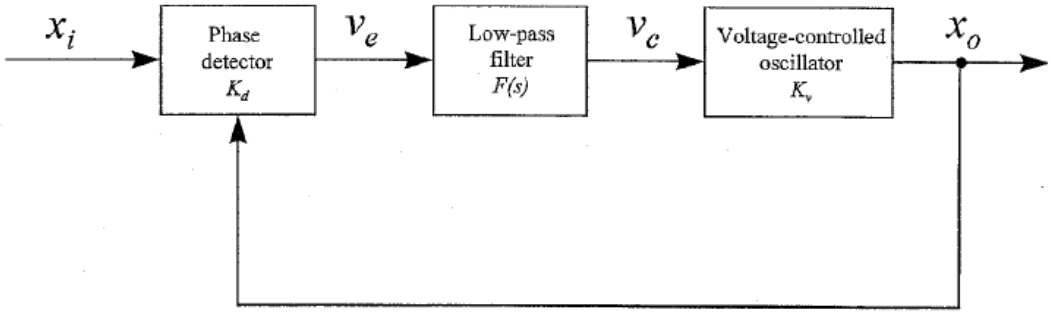

Figure 2.3. *A Basic structure of a phase-locked loop system. [13, p .2]*

2.2.5 U-f inverter control

Controlling inverter as a voltage source is based on emulating a synchronous machine by implementing frequency versus active power droop characteristics which is illustrated in figure 2.4.

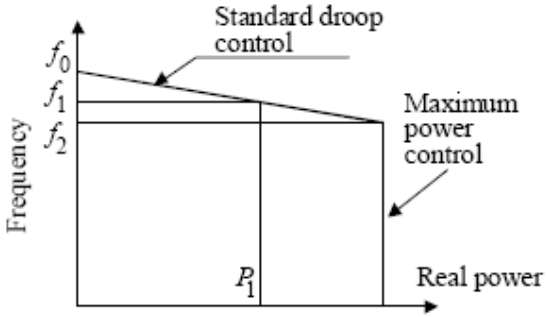

Figure 2.4. *Basic idea of droop characteristics in U-f inverter control. [14, p. 3]*

Angular output frequency of the inverter can be calculated as presented in equation (9).

$$\omega = \omega_0 - k_P \cdot P \quad (9)$$

In (9) P stands for active output power of the inverter, k_P is the droop slope and ω_0 is the idle value of angular frequency of the inverter output at no load conditions. [9, p. 3] With a grid connected inverter the output frequency is determined by the grid. In a standalone power system frequency of the island is determined by the load, i.e. as in figure 2.4 frequency f_1 corresponds to active power P_1. After reaching the maximum power provided by the primary energy source, system switches into constant power control acting on the phase shift between inverter fundamental voltage and the voltage measured from the point of common coupling, or PCC, and returns to follow droop characteristics when frequency f_2 is exceeded by some given factor. [14, p. 3] With this kind of localized control U-f is able to react to disturbances, mainly load changes, based

on information at its terminals and the operation is not dependent on communication between the DG units or centralized control system. [9, p. 4]

Controlling voltage amplitude at voltage source inverter output also resembles that of a synchronous machine. Output voltage can be calculated as stated in equation (10).

$$V = V_{nl} - k_Q \cdot Q \quad (10)$$

In (10) Q stands for reactive power output of the inverter, k_Q is the droop slope and V_{nl} is the idle value of voltage at the inverter output at no load conditions. The basic behavior of voltage versus reactive power drooping is similar to that of frequency versus active power presented in figure 2.4. [14, p. 3]

2.2.6 Switching between PQ – and U-f control modes

It is most likely that a transient will occur when a DG unit switches from grid connected PQ control mode into islanded U-f control mode. This is due to the fact that if the amount of generated power before grid failure does not match the loading of the islanded system, DG unit will find a new operation point according to frequency drooping characteristics. If the connected load is too large the inverter operates in maximum power control mode which forces the output voltage to slide with respect to the reference which can be used as an indicative signal for shedding less important loads. Also, if the maximum output current of the inverter is met by high demand of reactive current and inverter operates in maximum current control the fundamental of the output voltage is limited. This results in under voltage within the island which also can be used for load shedding. [14, p.4]

When the main grid is to be connected again with islanded system it can be done by simply closing the connection between them. This is possible due to absence of inertia within inverters which will cause them to rapidly adapt the frequency of the grid and synchronize by means of power frequency drooping. [14, p.4]

3 ISLANDING DETECTION METHODS

Islanding detection is required from any DG unit because of the risks related to operational island [1]. Islanding detection methods can be categorized broadly in local – and remote methods. In principle the difference is that remote methods detect the islanding on the utility side, and local methods detect islanding on the DG side of the grid. Classifying of islanding detection is illustrated in figure 3.1.

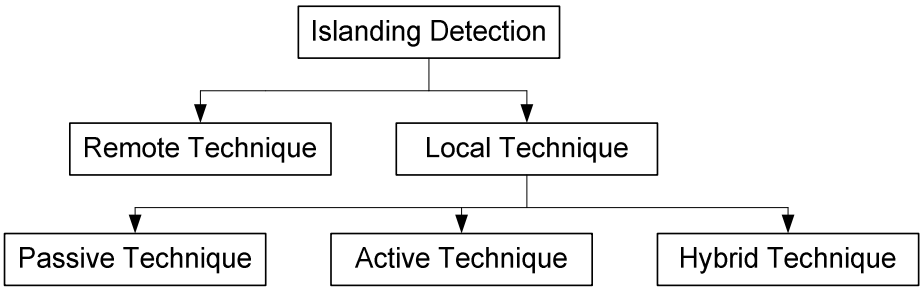

Figure 3.1. *Classification of islanding detection methods. [15, p. 2]*

Moreover, local islanding detection, in which this thesis is concentrating, can be divided into passive -, active – and hybrid islanding detection methods. [15, p.1] Behavior of an islanded power system is highly dependent on the construction of that system. E.g. a power system consisting synchronous machines behaves different to a power system operated by power electronics. In this thesis main concentration is in islanding of DG units operated by full power inverters. Since power system is subject to many kinds of transitions and disturbances an islanding detection method should not react to these situations [16, p. 2].

3.1 Non detection zone

Non detection zone, NDZ, is used as a performance index for islanding detection methods. A non detection zone is illustrated in figure 3.2. A non detection zone is presented in ΔP, ΔQ-plane and it illustrates the power – and reactive power mismatch within an island which is insufficient for islanding detection. The goal for any islanding detection method is to reduce non detection zone to zero. [16, p.1] In [17] it is recommended for distributed resources that a non-islanding inverter should cease to energize the utility in two seconds or less with all active-reactive power-balances. Effectiveness of an islanding detection method is dependent also on the absolute amount of reactive power produced and consummated in the power system. This is because reactive elements of a power system increase the probability to maintain adequate frequency after

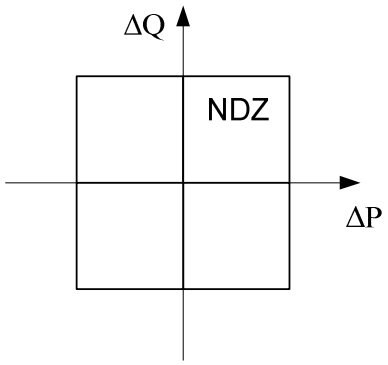

Figure 3.2. *A Non detection zone in ΔP, ΔQ-plane [16, p.2]*

islanding. Reactive power conditions within a power system can be referred to with quality factor, Q_f. Q_f relates active and reactive power of a power system also with corrected power factors. When power factor is usually observed at one point of a power system and derives from phase difference between voltage and current, Q_f takes into account also compensated reactive power within e.g. a distribution branch. Q_f is defined so that reactive power stored in the system is Q_f times the active power consumed in resistances of that system. [18, p. 3]

3.2 Passive islanding detection

Passive islanding detection is based on measurements such as voltage, frequency or harmonic content at DG PCC. Detection of an islanding situation is based on preset values of these electrical quantities being exceeded. Descriptive for passive islanding detection methods is that they do not affect the grid and thus, do not affect power quality of the DG and tend to have relatively large NDZs. [15, p.2]

3.2.1 Over/under voltage and over/under frequency

Islanding detection based on behavior of voltage and frequency is founded on the power and reactive power mismatch between the generation and loading of the islanded system. Power balances for e.g. within a distribution branch can be expressed as in (10) and (11).

$$P_{Grid} = P_{Load} - P_{DG} \quad (10)$$

$$Q_{Grid} = Q_{Load} - Q_{DG} \quad (11)$$

Behavior of the islanded system after the grid is disconnected depends on power – and reactive power balance within the island, P_{Grid} and Q_{Grid} respectively. Active power balance of a system consisting of inverter operated DG is directly proportional to the amplitude of voltage as in equation (12).

$$U'_{Isl} = \sqrt{\frac{P_{DG}}{P_{Load}}} \cdot U_{Grid} \quad (12)$$

In (12) U_{Grid} stands for voltage before islanding and U'_{Isl} stands for voltage after islanding. It can be seen that if there is more generation than loading within the island the voltage will increase and vice versa.

In addition to voltage amplitude, reactive power balance is related to frequency of the islanded system as stated in equation (13).

$$Q'_{Load} = Q_{DG} = \left(\frac{1}{\omega' L} - \omega' C\right) \cdot U'^{2}_{Isl} \quad (13)$$

Angular frequency of the islanded system can be derived from (13) yielding to (14).

$$\omega' = \frac{-\frac{Q_{DG}}{CU'^{2}_{Isl}} + \sqrt{\left(\frac{Q_{DG}}{CU'^{2}_{Isl}}\right)^{2} + \frac{4}{LC}}}{2} \quad (14)$$

It can be seen from equations (12) and (14) that smaller the amount of active or reactive power delivered from the main grid initially is, smaller the resulting change in amplitude of voltage and frequency of the system will be. Because of normal voltage and frequency variations in the grid the threshold limits for islanding detection has to be set relatively loose which results in large NDZs of this islanding detection method. Generally islanding detection based on voltage and frequency windows is considered insufficient to be used independently when there is a possibility that active – and reactive power production and consumption within that section of power system could be of a same magnitude. [16, p. 2]

3.2.2 Voltage harmonic monitoring

Monitoring of voltage harmonics can be used as an islanding detection method. The basic idea behind this method is to detect changes in harmonic content of the power system. It is possible to consider THD or only lower order harmonics, e.g. 3rd, 5th and 7th harmonic. Voltage harmonic monitoring is not considered a reliable islanding detection method since it is very difficult to find thresholds for detection of islanding situation. NDZ of this method depends strongly on the characteristics of loading within the island. I.e. reactive loading such as transformers will introduce low-pass characteristics which affect the harmonic content observed at the DG PCC. [16, p. 2]

It is possible to use a PLL structure for voltage harmonic monitoring. When voltage vector is synchronized to the rotating dq-frame it is possible to estimate frequency and amplitude of the voltage. To extract amplitude and frequency of the voltage exactly it is recommended in [16] to use a first order Butterworth filter. To be able to monitor different harmonics a harmonic synchronization PLL needs to be implemented. A PI controller is used to provide the fundamental frequency of the given harmonic and $d'q'$-frame synchronized to the given harmonic frequency is applied. The amplitude of the given harmonic is obtained from the calculation of V_d' and V_q' components. Usually no harmonics higher than 3rd, 5th and 7th order need to be considered in islanding detection. [16, p. 4]

3.2.3 Voltage unbalance monitoring

In islanding situation the DG unit has to take care of the islanded loads which will often result in voltage unbalance. Voltage unbalance can be calculated as in equation (15).

$$\mathrm{U_{UB}} = \frac{\mathrm{U_{Neg}}}{\mathrm{U_{Pos}}} \tag{15}$$

In (15) U_{Neg} and U_{Pos} stand for negative – and positive sequence voltages at DG PCC. Voltage unbalance monitoring can be used together with voltage harmonic monitoring. Voltage unbalance of three phase voltages and THD of one phase is calculated at predetermined sampling interval and then compared with threshold limit to determine islanding situation. Thresholds for this method are difficult to set and it will fail for high values of quality factor Q_f. [19, p. 2]

3.2.4 Phase monitoring

Monitoring phase angle between inverter terminal voltage and output current for a sudden change can be used as an islanding detection method. Though, it has to be noted that when PLL structure for grid synchronization is implemented in the inverter it is able to follow the grid so that voltage and current will always be in phase and thus islanding cannot be detected. [16, p. 2]

Phase monitoring, i.e. monitoring the voltage vector angle in relation to q-axis is able to detect islanding also with PLL applications. After every fundamental cycle, the angle between voltage vector and q-axis is stored and compared with the value during previous fundamental cycle. In other words, the change in the slope of the voltage angle when plotted in angle-time frame can be detected. Effectiveness of phase monitoring method is strongly dependant on the reactive elements within the power system since the change in voltage vector angle depends on the load resonant frequency. If the load is resonating at the fundamental frequency no shift in voltage vector angle is detected. Performance and NDZ of the method is similar to that of over/under frequency method and thus insufficient to be used as a primary islanding detection method. [16, p. 3]

3.2.5 Rate of change of frequency

Rather than monitoring the absolute value of frequency, the rate of change of frequency, or ROCOF, is more sensitive as an islanding detection technique. This technique is more suitable for power systems where there is synchronous generator supplying the island in parallel to inverter. In this case the thresholds for ROCOF are determined on basis of generator swing equation (16) which determines the rate of change of frequency.

$$\frac{\Delta \mathrm{f}}{\Delta \mathrm{t}} = \frac{\Delta \mathrm{Pf}}{2HP_{Nom}} \tag{16}$$

In (16) f stands for power system frequency and ΔP is the change in output power during time step Δt. H is the inertia constant of the generator and P_{Nom} the rated generating capacity. In figure 3.3 it is illustrated how the threshold of ROCOF is exceeded with a

negative change in frequency. From figure 3.3 it is also seen how the under frequency protection would fail to detect the islanding situation. [20, p. 2-3]

It is noted in [20] and [21] that there is problems with ROCOF in case of system disturbances which may result in false detection and unnecessary tripping of the DG unit. To overcome this, a method called comparison of rate of change of frequency, or COROCOF is suggested in [21]. This technique is based on comparing the rates of changes in frequency between all interconnected COROCOF relays. In case of a system disturbance the frequency is normally affected in the whole power system and CORO COF relays send a blocking signal to each other to avoid nuisance tripping. In case of an islanding the relay will not receive this signal and thus is permitted to trip if ROCOF threshold is exceeded. [21, pp. 1-2]

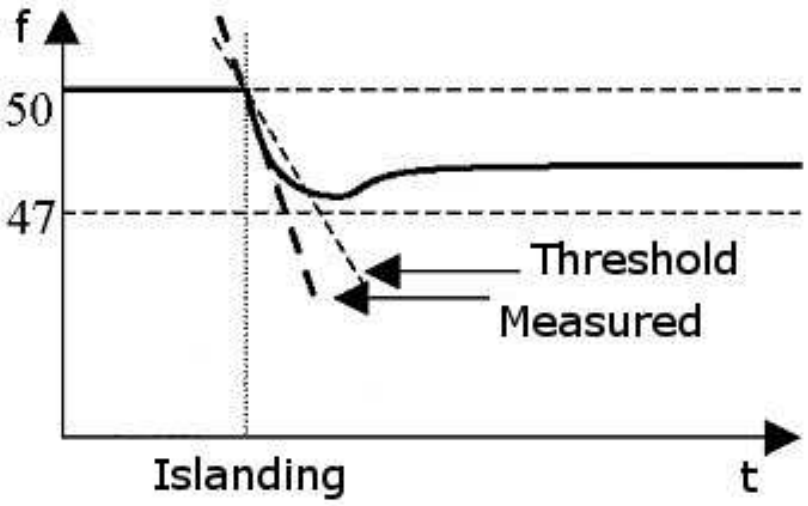

Figure 3.3. *ROCOF exceeding negative threshold. [20, p. 3]*

3.2.6 Rate of change of frequency over power

Monitoring the rate of change of frequency over power, $\frac{df}{dP}$ respectively, is a method developed in order to defeat the short comings of monitoring directly voltage amplitude and/or frequency. Also, rate of change of frequency over power has been studied to yield to better results in islanding detection than applications monitoring only rate of change of frequency or rate of change of power. To present the idea a synchronous machines operating DG containing distribution branch in which the power balance can be expressed as in equation (10) is considered. When the distribution branch is operating independently from the main network their frequency versus power characteristics can be expressed as in equations (17) and (18).

$$G_{Grid} = \frac{df_{Grid}}{dP_{Grid}} \tag{17}$$

$$G_{DB} = \frac{df_{DB}}{dP_{DB}} \tag{18}$$

In (17) and (18) P_{Grid} and P_{DB} are active power mismatches of the main network and distribution branch and f_{Grid} and f_{DB} represent frequencies of the systems. It is evident that G is inversely proportional to the generating capacity of the power system which results in that G_{Grid} will be significantly smaller than G_{DB}. If the distribution branch is connected to the main network, the change P_{Ch} in power transformed from main network to the distribution branch for a load change $P_{Ch-Load}$ within the distribution branch, can be expressed as in (19) and (20).

$$\frac{\mathrm{dP_{DB}}}{\mathrm{df_{DB}}} = \frac{\mathrm{dP_{Ch}}}{\mathrm{df_{DB}}} - \frac{\mathrm{dP_{Ch-Load}}}{\mathrm{df_{DB}}} \tag{19}$$

$$\frac{\mathrm{dP_{Grid}}}{\mathrm{df_{Grid}}} = -\frac{\mathrm{dP_{Ch}}}{\mathrm{df_{Grid}}} \tag{20}$$

Also, with interconnected systems frequencies has to be the same as in equation (21).

$$\mathrm{df_{Grid}} = \mathrm{df_{DB}} \tag{21}$$

With (20) and (21), (19) can be expressed as in (22).

$$\frac{dP_{DB}}{df_{DB}} = -\frac{dP_{Grid}}{df_{Grid}} - \frac{dP_{ch-Load}}{\mathrm{df_{DB}}} \tag{22}$$

By substituting (17) and (18) into (22) it is possible to calculate rate of change of frequency over power as seen from DG terminal when distribution branch and main network are considered as two interconnected networks. This yields to equation (23).

$$\frac{df_{DB}}{dP_{Ch-Load}} = \frac{-G_{Grid}G_{DB}}{G_{Grid}+G_{DB}} \tag{23}$$

In a situation where distribution branch is operated independently from the main network the rate of change of frequency over power for a given load change can be calculated as in (18). From (18) and (23) it can be seen that equal changes in active power will result in significantly different figures under different scenarios, i.e. grid connected and islanded operation yielding to an index to be used for islanding detection. [22, p. 2]

It is crucial to be aware of the effects of load changes in order to find thresholds for islanding detection. From DG terminal the rest of the power system can be viewed as an equivalent voltage source U_{Th} which is connected to DG through an impedance $R + jX$. When the voltage at the DG unit terminal is noted as U_{DG} the voltage difference ΔU between U_{Th} and U_{DG} and power P_{Tr} transferred between these voltage sources can be expressed as in equations (24) and (25).

$$\Delta \mathrm{U} = \frac{\mathrm{R(P_{DG}-P_{Load})+X(Q_{DG}-Q_{Load})}}{\mathrm{U_{DG}}} \tag{24}$$

$$\mathrm{P_{Tr}} = \frac{\mathrm{X(P_{DG}-P_{Load})+R(Q_{DG}-Q_{Load})}}{\mathrm{U_{DG}^2}} \tag{25}$$

It is seen that variation of $\mathrm{U_{Th}}$ will result in variation of $\mathrm{U_{DG}}$ amplitude and frequency which in case of a synchronous generator leads to a change in power fed into network from the DG unit. From this it can be conducted that voltage amplitude and frequency are influenced mutually and depending on the reactive/active power balance the variation of the system frequency will result in load change. [22, p. 3]

It should be noted that a DG unit with full power converter grid interface will act differently than a synchronous machine. I.e. variations in amplitude and frequency of

the voltage at DG terminal will not naturally initiate a change in reactive – or active power output of the unit.

3.3 Active islanding detection

The difference in principal between active and passive islanding detection is that active methods introduce perturbations such as injecting reactive current into the grid in order to detect islanding situation. Moreover, active methods can be divided into two main categories, transient methods and steady-state methods. Transient methods generate a transient current into power grid and measure the response of the grid, namely voltage and current before and after the transient injection. Steady state methods inject a known and usually periodic disturbance to the grid from which analyses are derived for steady state situation. Active methods are developed in order to overcome shortcomings of passive methods such as large NDZs. Downside is that active methods may affect the power quality negatively. Also, some active methods are very complex and thus difficult to be implemented into inverter control system. Such an implementation is also difficult to test and verify as well as separate the functionality from other features of the inverter. [1; 23, p. 1; 24, p. 2]

3.3.1 Detection of impedance by harmonic injection

By injecting a current harmonic with a specific frequency into PCC of a DG unit it is possible to detect the equivalent impedance of the grid. A monitoring PLL is designed to detect variations in voltage at the frequency of the current injected by the inverter. Various methods for determining grid equivalent impedance by harmonic injection are presented in literature from which some require dedicated measuring and calculation equipment. This section focuses on one presented in [24] which is stated to be implementable into a DG inverter. [23; 24; 25]

Choosing of frequency of the injected harmonic or sub-harmonic current depends on the calculation methodology used. By using a frequency close to fundamental the impedance at the injected frequency can be assumed to be close to that at the fundamental frequency. [23, p. 2] In [25] a frequency ten times the fundamental is used and the grid equivalent impedance is determined by means of linear interpolation. Choosing of the frequency should be done avoiding resonant frequency of the grid and with respect to the interaction with resonance of the current controller. [25, p. 3]

Major challenge in impedance detection by harmonic injection is to measure current-voltage response when the system is energized, loaded and the DG unit is supplying active power to the grid. If using system characteristic harmonic frequency it has to be taken into account when determining impedance. System characteristic frequency depends on the used inverter topology. For a six pulse inverter characteristic harmonics can be calculated as $h = n \cdot 6^{+}_{-}1$, where $n = 1,2,3$ ... and h is the running number of a harmonic. Frequency of the given harmonic is hth multiple of the fundamental frequency. Use of characteristic frequency leads to analyzing the grid as a complex model

which has to be divided into individual frequency planes containing both the background distortion of the grid and harmonic distortion generated by the consumers. One solution to this is to measure background distortion in prior to current injection which then can be subtracted from measurements. This solution makes a hypothesis that background distortion does not change between the measurements. It is evident that using system characteristic harmonics requires a lot of processing power and memory and thus will be difficult to implement in a DG inverter. [24, p. 2]

Principle of the method presented in [24] is to inject non-characteristic harmonic current into the grid with DG inverter. The current injection is done by adding a harmonic voltage to the voltage reference of the inverter. Resulting voltage and current are measured with sensors already resident in the inverter for normal operation purposes. Measured quantities are processed by means of Fourier analysis for the used frequency which results in current, I_h, and voltage, U_h, at the injected frequency as in equation (26). Obtained voltage and current can be divided into real – and imaginary parts as in equation (27) from which the complex impedance at the given frequency can be calculated as in equation (28).

$$Z_h = \frac{U_h}{I_h} \tag{26}$$

$$Z_h = \frac{U \cdot e^{j\varphi_V}}{I \cdot e^{j\varphi_I}} = Z_h \cdot e^{j\varphi Z} \tag{27}$$

$$Z_h \cdot e^{j\varphi Z} = R_G + j\omega_h L_G \tag{28}$$

In above equations Z_h stands for grid equivalent impedance consisting of equivalent resistance R_G and inductance L_G. U and I stand for voltage and current, respectively, φ for complex angle in radians and ω_h for angular frequency of the given harmonic. If the impedance is assumed to be linear equation (29) can be used to obtain the grid equivalent impedance at the fundamental frequency.

$$Z_f = R_G + j\omega_f L_G \tag{29}$$

Choosing the length of time which the harmonic injection is applied, how often it is done and amplitude of the injected harmonic is difficult and empirical data should be used to determine parameters for acceptable operation. It has to bear in mind also that injecting harmonic content into grid effectively decreases the power quality at PCC. [24, p.3]

After the DG inverter injects harmonic current and the response is measured with voltage and current sensors the discrete Fourier transform, DFT, is used to obtain voltage and current amplitude and phase at the given frequency. Equation (30) is used by DFT to calculate coefficients for the Fourier series of voltage and current harmonic.

$$\bar{\Lambda}_h = \sum_{n=0}^{N-1} \chi(n) \cdot cos\left(\frac{2\pi hn}{N}\right) - j \sum_{n=0}^{N-1} \chi(n) \cdot sin\left(\frac{2\pi hn}{N}\right) \tag{30}$$

In (30) *N* stands for samples in fundamental period and $\chi(n)$ is voltage or current quantity at given *n*. $\bar{\Lambda}_h$ represents the complex Fourier vector of the *h*th harmonic of voltage or current. In figure 3.4 a vector approach to calculating real – and imaginary parts of the impedance is illustrated. It is noted in [24] that this kind of approach consumes

much DSP resources and thus, should be avoided. A better solution from DSP point of view is so called running-sum approach which is illustrated in figure 3.5 [24, pp. 3-4]

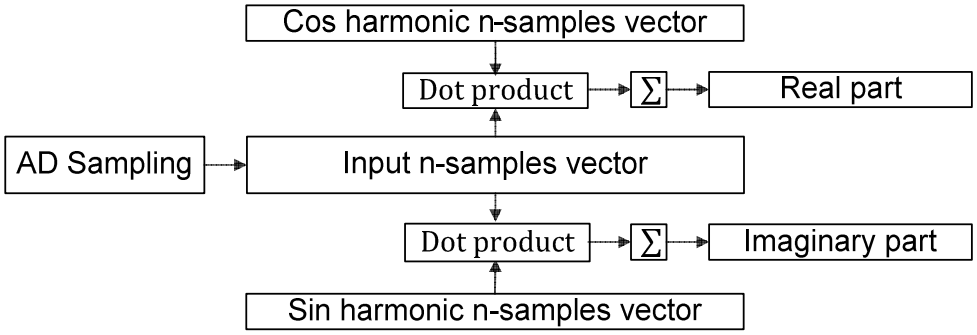

Figure 3.4 *A Vector approach to determining impedance on basis of sampled complex vector. [24, p. 3]*

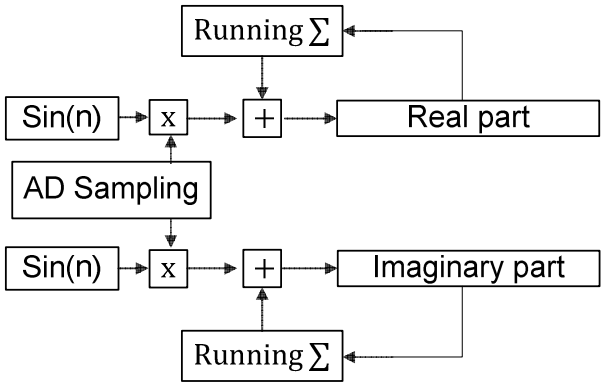

Figure 3.5 *A Running-sum approach to determining impedance on basis of a sampled complex vector. [24, p. 4]*

Simulation and experimental testing of described method is carried out in [24]. It is concluded that inaccuracy of the estimation of impedance after introduction of three seconds moving average filter to eliminate random errors and sampling flickering is less than 10%. Current injection is done at 75Hz into 50Hz grid to be able to justify the linearity assumption of impedance. Amplitude of 1,5A for the injected current is chosen as a compromise between accuracy and to avoid increasing THD. 1,5A is 11,5% of the 13A nominal current of the inverter resulting in 1,8V or 0,8% harmonic voltage component at 75Hz. Because of this the effect of the injection on THD is evident. However, effect on other harmonic content than that of 75Hz is negligible. Also selection of repetition rate, i.e. how frequently the injection is done has to be done carefully. It is an optimization problem between the performance of islanding detection and THD. A Repetition rate of 1/14 is considered optimal in [24] which means that a period of 75Hz current is injected once every fourteenth fundamental period. This results in internal delay of 280ms for islanding detection with 50Hz fundamental frequency but the actual delay

of islanding detection depends also on the used moving average filter and time used for calculating the grid equivalent impedance.

Islanding detection with harmonic injection is based on the voltage response dependency on grid equivalent impedance, i.e. the relation of voltage and current. To be able to conclude islanding from this a predetermined limit for the change in grid equivalent impedance to be interpreted as islanding has to be set. Effectiveness of actual islanding detection is not considered in [24] but it is stated that inaccuracy of 10% in impedance estimation is acceptable in EN 50330-1. [24, pp. 2-7] Limitations of this method relate to accuracy of a DG inverter's voltage measurement and the possibility that linearity assumption of impedance is not justified. Also the threshold for the efficient islanding detection without nuisance tripping might be difficult to obtain especially in weaker grids, i.e. grids with greater equivalent impedance, or in grids where impedance changes occur naturally because of changes in grid configuration.

3.3.2 Active power variation

In islanding condition the response of the grid to changes in active power is more sensitive than during grid connected operation. Active power variations when operating in an island with inverter grid interfaced DG units affect directly the voltage at the point of common coupling. When the power system involves synchronous machines with governor and excitation control active power variations result in variations of frequency. Dependence of active power produced by the DG unit and thus consumed by the island loading can be expressed as in equation (34) which is derived through (31)-(33).

$$P_{DG} = P_{Load} = 3\frac{U_{Ph}^2}{R} = \frac{U_{LL}^2}{R} \tag{31}$$

$$U_{LL} = \sqrt{RP_{DG}} \tag{32}$$

$$\frac{\delta P_{DG}}{\delta V} = 2\frac{U_{LL}}{R} = 2\frac{\sqrt{RP_{DG}}}{R} = 2\sqrt{\frac{P_{DG}}{R}} \tag{33}$$

$$\Delta U_{LL} = \frac{\Delta P_{DG}}{2}\sqrt{\frac{R}{P_{DG}}} \tag{34}$$

In equations (31)-(34) P_{DG} stands for generation and P_{Load} for active power consumed in the resistance R within the island. U_{Ph} and U_{LL} stand for phase-to-ground and phase-to-phase voltages at PCC. By varying the output power of the DG unit it is possible to carry the voltage amplitude out of the range of normal operation in order to cause the over/under voltage detection to trip. [23, p. 2] Active power variation is a simple but not very effective method for islanding detection. E.g. according to equation (34) in an island constituting 1kW of three-phase active power production with 400V main voltage, the additive production to achieve 110%, 440V, in voltage would be 200W. I.e. 20% increase in production results in 10% increase in voltage. Traditionally there is no reserve in the production rate of DG for this as it is dependent on the intensity of the primary energy source. Reducing the produced power would be possible but it would have to be done rather frequently and fast in order to detect islanding in adequate time. This would possibly result in transients and flickering during normal operation of the DG

unit depending on its size and grid configuration. Also, a dip in voltage could be interpreted as a grid fault rather than islanding with DG units equipped with FRT functionality. If the rate of change in active power is slower it would reduce the produced energy which is not desired and islanding detection would be slow.

3.3.3 Sandia voltage shift

Sandia voltage shift, or SVS, is based on amplifying changes in grid voltage amplitude by introducing a positive feedback from voltage amplitude to inverter output current. Voltage fluctuations are determined on basis of difference between filtered average amplitude and cycle by cycle measurement of the voltage amplitude. In case of islanding the voltage amplitude should be carried out of the permitted operating window causing over – or under voltage protection to trip. [26, p. 21] Threshold for detection of islanding with SVS has to be done case by case since the response in voltage amplitude to current is dependent on the grid configuration. Also, when it is possible that grid configuration changes, e.g. a backup connection is used in order to secure continuity of supply a different threshold needs to be used. When grid is connected the effect of changes in current amplitude on voltage amplitude should remain under the threshold. Slight drawback in power quality and inverter efficiency can be considered as weaknesses of SVS. Usually SVS is implemented together with Sandia frequency shift when they combine a very effective islanding detection method. [19, p. 4]

3.3.4 Reactive power variation

Similarly to that between voltage and active power, the dependence of frequency and reactive power can be used to detect islanding situations. Simplest solution is to monitor the difference between frequency f of voltage at the PCC and nominal frequency f_n. This difference is amplified by gain K_f to provide reference for additional reactive power dQ as in equation (35).

$$dQ = K_f(f_n - f) \tag{35}$$

Thus, positive feedback is exploited to cause the frequency to drift out of the acceptable range and under/over frequency protection to trip. [23, p. 3] It is noted that the direct dependence of frequency and reactive power is true only in power systems fed solely by inverters. If there are also synchronous machines maintaining frequency and participating in voltage control, changes in system reactive power resulting in changes of voltage level will be compensated by the machine's excitation control and reactive power balance is maintained without influencing the frequency.

3.3.5 Active frequency drift

Active frequency drift, AFD, operates with the waveform of the inverter output current. A dead time during which the inverter output current is zero is set before grid voltage zero crossing as in figure 3.6 is illustrated. In an islanding situation the voltage frequen-

cy at PCC will start to follow the current frequency and force it to drift up or down causing under/over frequency protection to trip.

Because the reference for the output current of an inverter with AFD method contains the dead time it follows that there is a phase shift between the fundamental component of the inverter output current and grid voltage as in figure 3.6 is illustrated. The dead time is related to phase shift with a chopping fraction cf as in equation (36) from which the equation describing dead time in figure 3.6 is derived. [23, p. 2] Relation of angular frequency ω of the grid voltage fundamental and output current fundamental component's equivalent angular frequency ω' is expressed in (37). [27, p. 2]

$$\varphi_d = \frac{cf \cdot \pi}{2} \tag{36}$$

$$\omega' = \frac{\omega}{1-cf} \tag{37}$$

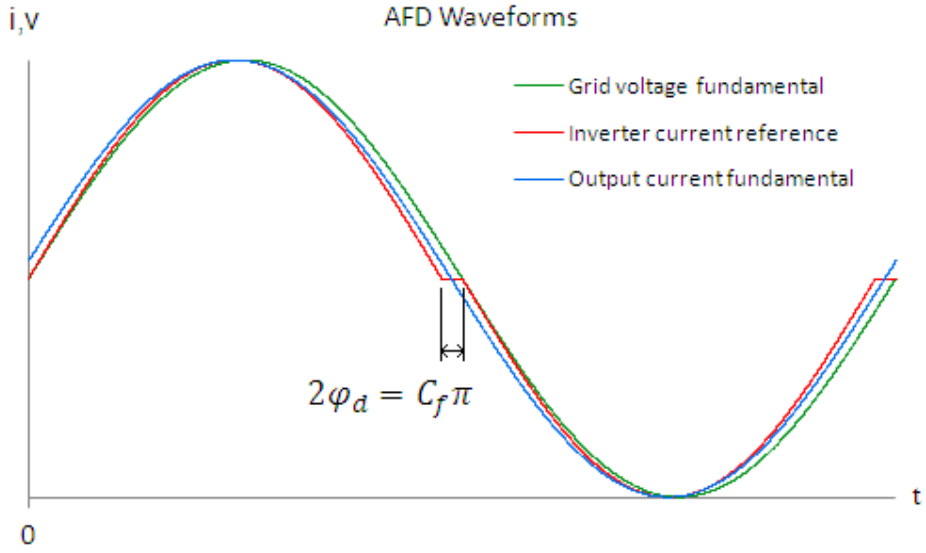

Figure 3.6 *Current waveforms in active frequency drift. [27, p. 2]*

Considering the voltage phase at PCC as a reference the output current of an inverter without AFD perturbation can be expressed as in equation (38).

$$i_{ref}(t) = \sqrt{2} I_{RMS} \sin(\omega t) \tag{38}$$

In (38) I_{RMS} is the RMS value of current and $\sqrt{2}I_{RMS}$ can be expressed as a maximum value of current i_{max}. With the distortion introduced by AFD the inverter current reference becomes discontinuous and can be expressed as in equation (39).

$$i_{ref-AFD}(t) = \begin{cases} i_{max} \sin\left[\omega'\left(t - \frac{n\pi}{\omega}\right)\right] & \frac{n\pi}{\omega} \le t \le \frac{n\pi}{\omega} + \frac{\pi}{\omega'} \\ 0 & \frac{n\pi}{\omega} + \frac{\pi}{\omega'} \le t \le \frac{(n+1)\pi}{\omega} \end{cases} \tag{39}$$

In (38) n is an integer 1, 2, 3… Equation of the fundamental output current of the inverter (40) with AFD perturbation is similar to (38) but with a phase shift φ_d.

$$i_1(t) = i_{max} \sin(\omega t + \varphi_d) \tag{40}$$

Drawbacks of AFD are an increase in THD and the fact that a constant phase difference between voltage and current will affect reactive power control. This will ex-

clude AFD form applications where unity power factor control or grid voltage support is required. Effectiveness of AFD is an optimization problem between NDZ and undesirable effects.

3.3.6 Active frequency drift with pulsating chopping fraction

AFD method has been developed further to increase power quality and effectiveness of islanding detection. In [28] an AFD method with pulsating chopping fraction, AFDPCF, is introduced. Pulsation of chopping fraction is illustrated in figure 3.7 and chopping fraction for AFDPCF is expressed in equation (41).

$$\mathrm{cf} = \begin{cases} \mathrm{cf_{max}} & \text{if } \mathrm{T_{cf-max}} \\ \mathrm{cf_{min}} & \text{if } \mathrm{T_{cf-min}} \\ 0 & \text{otherwise} \end{cases} \tag{41}$$

In (41) maximum and minimum for chopping fraction, $\mathrm{cf_{max}}$ and $\mathrm{cf_{min}}$, respectively, and their on-times are stated.

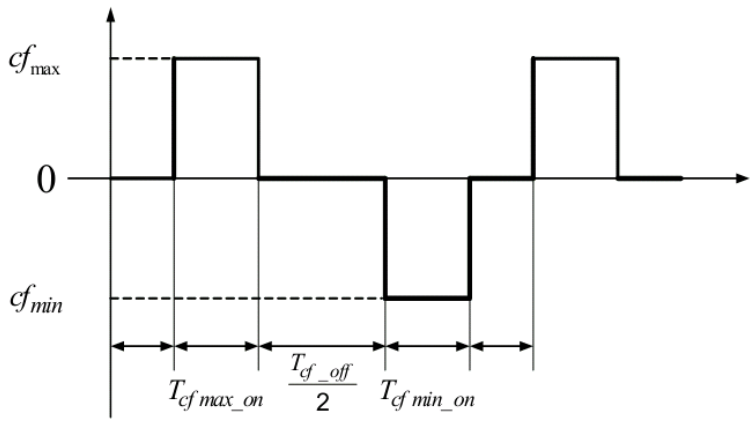

Figure 3.7. *Chopping fraction is pulsating between minimum and maximum values.* $\boldsymbol{T_{cf\_off}}$ *stands for time that* $\boldsymbol{cf}$ *remains zero during one pulsation cycle. [28, p. 3]*

Pulsation of chopping fraction between positive and negative values will make the phase shift introduced in equation (36) also alternate between positive and negative. This makes the inverter output current fundamental component lead or lag the voltage fundamental with respective period.

Since there is a direct relation between chopping fraction and total harmonic distortion the determination of cf should be done according to THD. According to standardization [29] it is stated that current THD shall be less than 5%. Requirements in other standards are similar. The relation between cf and THD is illustrated in figure 3.8. It can be seen that in order to maintain acceptable THD level the minimum value for cf is -0,045 and maximum value is 0,046. This will result in THD level remaining under 5%. It is noted that with cf value zero, i.e. AFD method inactive, THD is 0,89%. This is unreachable with MW-class converters since the THD during normal operation is at a level of 3-4%. Higher THD during normal operation will limit the absolute value of chopping factor to be smaller than that suggested [28].

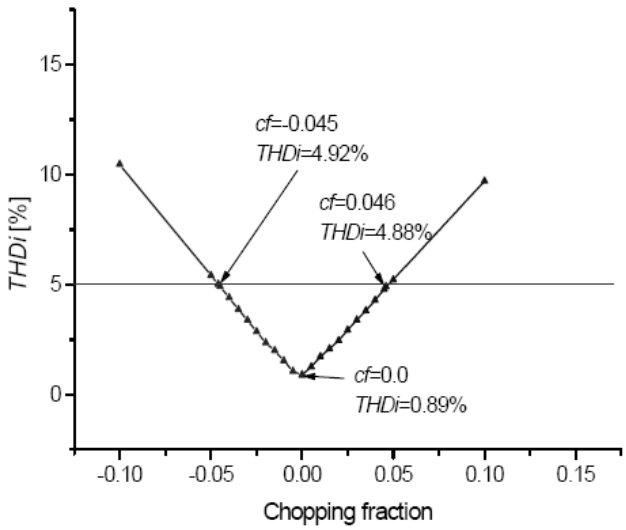

Figure 3.8. *The relation between chopping fraction and current total harmonic distortion.[28, p. 3]*

It is shown mathematically in [28] that AFDPCF is able to detect islanding situation in maximum of 1,4s within PCC grid conditions suggested in [29] and only PQ-controlled inverters connected within the island. Accepted grid conditions at PCC are stated to be within voltage range $88\% < U_{Nom} < 110\%$ and frequency range $59{,}3Hz < f_{Nom} < 60{,}5Hz$ for DG units under 30kW. [27, pp. 3-4] Voltage and frequency limits for acceptable grid conditions vary slightly in different countries but are comparable with the ones stated in [29] which applies for distributed generation in USA.

3.3.7 Active frequency drift with positive feedback

An AFD method using positive feedback, AFDPF, offers improvement over AFD by increasing the deviation of frequency. Implementation of positive feedback results in smaller NDZ of islanding detection and thus, makes the detection more effective. This method is also referred to as Sandia frequency shift or SFS. Chopping fraction for AFDPF is expressed in equation (42).

$$\mathrm{cf_k} = \mathrm{cf_{k-1}} + \mathrm{F}(\omega_{\mathrm{k-1}} - \omega_{\mathrm{k}}) \quad (42)$$

In (42) cf_{k-1} and ω_{k-1} are chopping fraction and angular frequency during previous voltage cycle. F is a function of sampled frequency error. In [30] a linear function is used but it is noted that many other choices are possible. In addition to adding sensitivity to AFD, AFDPF has an advantage in that if the frequency of the islanded system starts initially decreasing the frequency error becomes negative. This results in that the output frequency of the inverter will reinforce this trend rather than counteracting to it as would be possible with AFD. It is also noted in [30] that AFDPF has potential to perform satisfactorily with multiple inverters connected in the islanded system. This is because AFDPF will amplify any deviation in frequency, be it, introduced by another inverter. [30, pp. 5-6] It is possible that during power system disturbances not leading to

islanding AFDPF has a possibility to amplify the disturbance by affecting the reactive power balance and thus, excitation control of synchronous machines leading in worst case to power system instability.

3.3.8 Slip mode frequency shift

Slip mode frequency shift, or SMS, is also referred to as slide mode frequency shift. SMS is based on making the phase of the inverter output current deviate from the voltage phase at PCC as a function of frequency error. Frequency error is the difference between nominal and actual frequency of the grid voltage. This principle will work as a positive feedback which in case of an islanding will push the grid frequency out of the limits of acceptable conditions for operation. [31, pp. 1-2] The difference between AFD methods and SMS is in that AFD methods introduce a dead time in inverter output current affecting the frequency of an islanded system and SMS modifies directly the inverter output current starting angle. With both methods the islanding is prevented by under/over frequency protection. [32, p. 1]

When the grid is connected the output current of the inverter can be expressed as in equation (43).

$$i = \sin(2\pi ft + \Theta_{SMS}) \tag{43}$$

In (43) f stands for frequency of voltage at PCC and θ_{SMS} is the phase angle for SMS method. θ_{SMS} is a sinusoidal function of the frequency error as in equation (44) and is plotted in figure 3.9.

$$\Theta_{SMS} = \Theta_{Max} \sin\left(\frac{\pi}{2} \frac{f - f_{Nom}}{f_{Max} - f_{Nom}}\right) \tag{44}$$

In (44) θ_{Max} is the maximum phase angle in radians and f_{Max} is the frequency at which θ_{Max} occurs. F_{Nom} is the nominal – and f the actual frequency at the PCC. [33, p. 2]

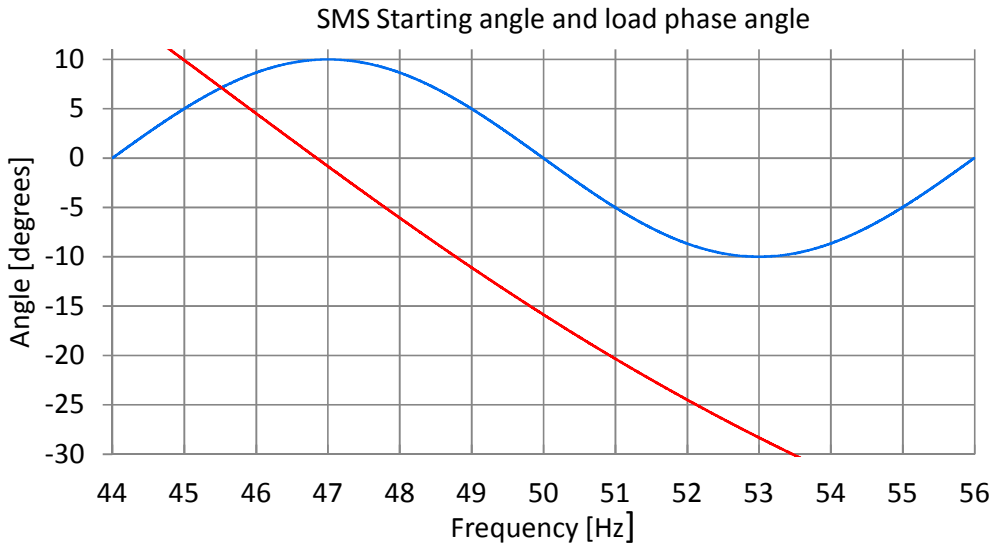

Figure 3.9 *Additive phase angle Θ_{SMS} for inverter output current in SMS method presented with red and phase angle φ_{RLC} of a passive RLC load in which $R = 10\Omega, L = 15{,}6mH$ and $C = 740\mu F$ presented in blue. [32, p. 2]*

In [32] it is shown mathematically that there is a load condition at which SMS method will maintain stable operation also during islanding. Phase angle for a parallel RLC load is determined as in equation (45) and plotted in figure 3.9.

$$\varphi_{\mathrm{RLC}} = -\tan^{-1}\left(\mathrm{R}\left(2\pi\mathrm{fC} - \frac{1}{2\pi\mathrm{fL}}\right)\right) \tag{45}$$

In (45) R, L and C represent resistive, inductive and capacitive components of the load and f stands for system frequency. Phase angle of a passive load is the angle between voltage and current. This phase angle also serves as a starting angle of the inverter output current with SMS. From this value the starting angle of the inverter current will start drifting away as a function of its frequency. If the changing rate of φ exceeds that of the starting angle, a stable operation point in which the islanding will not be detected, exists. Thus, the non-detection problem of SMS method derives from the fact that load phase angle is frequency dependent. [32, p. 2]

3.3.9 Automatic phase shift

To overcome problems with SMS method's stable operating points a method called automatic phase shift, or APS, has been suggested in [32]. The basic idea is to change the starting angle of inverter output current while the frequency remains nominal and introduce an additional phase shift which is applied once the steady state frequency is reached. Starting angle of kth inverter output current cycle with APS can be expressed as a linear function of voltage frequency and change in starting angle during previous cycle as in (46).

$$\Theta_{\mathrm{APS(k)}} = \frac{1}{\alpha}\frac{\mathrm{f_{k-1}} - \mathrm{f_{Nom}}}{\mathrm{f_{Nom}}} \cdot 360° + \Theta_{\mathrm{Add(k)}} \tag{46}$$

In (46) α is a scaling factor. The additional phase shift of Θ_{Add} is applied on basis of the change in steady state frequency Δf_{ss} and expressed in equation (47).

$$\Theta_{\mathrm{Add(k)}} = \Theta_{\mathrm{Add(k-1)}} + \Delta\Theta \tag{47}$$

In (47) $\Delta\Theta$ is a coefficient whose sign is determined on basis of the change in system steady frequency as in equation (48). [32, pp. 2-3]

$$sign(\Delta\Theta) = \begin{cases} \text{positive}, & \Delta\mathrm{f_{ss}} > 0 \\ \Delta\Theta = 0, & \Delta\mathrm{f_{ss}} = 0 \\ \text{negative}, & \Delta\mathrm{f_{ss}} < 0 \end{cases} \tag{48}$$

It is seen that $\Theta_{\mathrm{Add(k)}}$ becomes nonzero when the grid frequency differs from nominal and a phase shift between output current and grid voltage is always present when the grid frequency differs from nominal, also during normal operation. This is the shortcoming of APS method and effectively excludes it from applications in which the DG unit should be able to take part in grid voltage control or maintain unity power factor. In [32] a stable operating point is defined as that the variation in period of the voltage is smaller than 0,2ms for ten cycles. In $50Hz$ grid this results in frequency variation of $\pm 0{,}5Hz$ during 200ms. This high accuracy might be difficult to achieve with normal inverter controller and measuring equipment. After it is concluded that steady state frequency has changed, step changes in $\Theta_{\mathrm{Add(k)}}$ provided by $\Delta\Theta$ will in an islanding situa-

tion guarantee that the frequency keeps deviating until upper or lower frequency limit is reached and inverter tripped. [32, pp. 3-5] In [33] it is noted that determining every stable operation point might prove to be difficult and finding suitable $\Delta\Theta$ is problematic due to achieving small enough phase shift during normal operation and on the other hand introducing large enough phase shift to guarantee prevention of islanding situation. [33, p. 2]

3.3.10 Adaptive logic phase shift

Adaptive logic phase shift, or ALPS, is further development of SMS and APS algorithms to add robustness and sensitivity and to decrease effects of islanding detection on power quality during normal operation. In contrast to APS using grid nominal frequency when calculating starting angle for inverter current, ALPS uses measured average voltage frequency at PCC.

The difference in periods between inverter output current, i.e. the average of previous $N/2$ voltage periods, and last period of voltage is used as reference value for inverter output current starting angle and can be expressed as in (49). T represents the length of a voltage period and average for the period length T_{Av} is defined as in (50).

$$\Theta_{\mathrm{ALPS(k)}} = \pi \cdot \frac{\mathrm{T_{Av(N/2)} - T_{(k-1)}}}{\mathrm{T_{(k-1)}}} \tag{49}$$

$$\mathrm{T_{Av}} = \frac{1}{\mathrm{N}} \sum_{\mathrm{i=k-N}}^{\mathrm{k-1}} \mathrm{T(i)} \tag{50}$$

During next N periods the relationship between phase shift Θ_{ALPS} and its influence on the next period is evaluated. In islanding condition it is likely that if Θ_{ALPS} is greater than zero, i.e. voltage period has shortened, also the next period for voltage will be shorter than T_{Av} and vice versa. In [34] this is referred to as the probability of cause and effect. The probability of cause and effect relates the phase shift and the next period and is defined as in (51) or (52).

$$\begin{cases} \text{if} & \Theta_{\mathrm{ALPS}} > 0 \\ \text{then} & \Delta\mathrm{T} = \mathrm{T_{Av}} - \mathrm{T(k)} > 0 \end{cases} \tag{51}$$

$$\begin{cases} \text{if} & \Theta_{\mathrm{ALPS}} < 0 \\ \text{then} & \Delta\mathrm{T} = \mathrm{T_{Av}} - \mathrm{T(k)} < 0 \end{cases} \tag{52}$$

The probability of cause and effect is used as an indicator to introduce an additional phase shift as in (47) when a predetermined threshold is exceeded. Additional phase shift is added to Θ_{ALPS} while T_{Av} remains at its previous value and islanding is prevented when frequency is carried to trip limit. When additional phase shift Θ_{Add} is nonzero voltage period average value is monitored for every N/2 series. If the difference between two consecutive $N/2$ averages is small for two consecutive times or the probability of cause and effect is below the threshold, Θ_{Add} is set to zero and T_{Av} calculation is initiated again. In [34] simulations and testing of the proposed method is carried out and it is stated that ALPS is very effective islanding detection method with minimal increase in THD during normal operation. [34, pp. 2-4] Also, it does not affect reactive power control.

3.4 Hybrid islanding detection

Hybrid islanding detection methods are combinations of passive and active islanding detection techniques. Hybrid methods are developed in order to combine advantages of active and passive methods such as unaffected power quality during normal operation and small NDZ. In literature there are multiple suggestions for parameters which would best suit for monitoring and modulation in islanding detection applications.

3.4.1 Voltage unbalance and frequency set point

In [35] a hybrid method combining monitoring of voltage unbalance and varying frequency set point is proposed. Method is designed for DG units operating with synchronous generators but is stated to be implementable also for non-synchronous DG in microgrids with low penetration of DG. Idea is to monitor voltage unbalance and especially spikes in it. Voltage unbalance here is the relationship of voltage positive – and negative sequences. Threshold for maximum allowed spike in voltage unbalance is suggested to be 35 times the average unbalance during previous one second. These are empirically chosen values. After the threshold is exceeded the frequency set point is lowered gradually, e.g. 1Hz during one second. After changing the frequency set point the voltage frequency at PCC is monitored for e.g. 1,5 seconds and if there is a large enough change it is conducted that islanding has occurred. If there is none or negligible change in voltage frequency the frequency set point is changed back to nominal and operation is continued. [35, pp. 2-3]

It is noted to be an advantage of this technique that the impact on power quality is small. This is due to the facts that during normal operation there is not any disturbances introduced to the grid and it is noted that in case of disturbances such as load switching only the DG units connected to the same distribution branch with the load are reacting to the situation by lowering their frequency set point instead of all the DG units trying to destabilize the grid at the same time. Also, this technique permits the autonomous operation of DG unit after islanding detection. [35, p. 5] Drawbacks of this technique relate to difficulties of finding suitable thresholds for islanding detection and not to cause nuisance tripping. Also a situation in which there is a transient in frequency but voltage levels remain within acceptable limits would go undetected.

3.4.2 Covariance of current and voltage periods and adaptive reactive power shift

In [36] a method combining the covariance between commanded current period and PCC voltage period and reactive power variation is used as an islanding detection index. The relationship between the periods T of inverter output current and PCC voltage can be defined as in (53) where subscripts u and c stand for voltage and current and φ is the phase angle between current and voltage.

$$\mathrm{T}_u = \frac{1+\varphi}{2\pi} \cdot \mathrm{T}_c \tag{53}$$

When inverter is in grid connected operation there is negligible correlation between commanded current period and measured voltage period. In case of an islanding this relationship comes nearly linear as the voltage frequency will follow the commanded current frequency. To avoid false detections caused by noise in the measured voltage period a moving average filter of four voltage cycles is used as the commanded current period. Noise in the measured voltage period can be caused by natural deviations in system frequency or unideality in measuring the periods. Covariance. i.e. how the periods of current and voltage depend on each other is presented in equation (54).

$$\mathrm{Cov}(\mathrm{T_{av}}, \mathrm{T_v}) = \mathrm{E}[(\mathrm{T_{av}(n)} - \mathrm{U_{av}}) \cdot (\mathrm{T_v(n)} - \mathrm{U_v})] \quad (54)$$

In (54) u_{av} and u_v stand for the mean of average of previous four voltage periods and voltage period, T_{av} and T_v, respectively. E stands for expectation value. [36, pp. 2-3]

After the covariance index exceeds its threshold the active method to be applied is adaptive reactive power shift, or ARPS. This method is in principle similar to ALPS technique referred in chapter 3.3.10. The difference is that ARPS shifts the d-axis current instead of current phase. The shift of d-axis current is expressed in equation (55).

$$\mathrm{i_{d(k)}} = \mathrm{K_d} \frac{\mathrm{T'_{av}} - \mathrm{T_{v(k)}}}{\mathrm{T_{v(k)}}} \quad (55)$$

In (55) K_d is a gain which is suggested to be chosen so that d-axis current variation is less than one percent of q-axis current in grid connected operation. Determining both K_d and threshold for covariance index is to be done based on empirical data. The shift in d-axis current is applied according to same principle as additional phase shift in ALPS. The probability of cause and effect is monitored and when the threshold is exceeded $i_d(k)$ is applied to accelerate the phase shift action leading to rapid change in system frequency and causing the under/over frequency protection to trip. When combining the covariance index monitoring and ARPS it is suggested in [36] to keep the ARPS technique active 8 cycles as long as the covariance index is greater than preset threshold. [36, pp. 4-6]

3.4.3 Grid impedance estimation

In [37] an algorithm for estimating grid impedance and equivalent voltage source is presented. The algorithm is based on three phase current and voltage measurements which are transferred into dq synchronous reference frame. The frame is synchronized with the frequency of the grid provided by PLL. The voltage and current measurements after balancing and noise removal are the input signals for the estimation algorithm. I.e. the negative sequence of voltage is removed from the measurements to comply with symmetrical grid model and noise is filtered out. [37, p. 2]

For description of the estimation process a three phase inverter delivering active power P and consuming reactive power Q with instantaneous phase voltages $\mathrm{v_a}, \mathrm{v_b}$ and $\mathrm{v_c}$ and phase currents i_a, i_b and i_c is considered. In a steady state operation the operation point can be described as in equation (56).

$$\mathbf{V} = \mathbf{I} \cdot \mathbf{Z} + \mathbf{E} \quad (56)$$

In (56) **V** represents phase voltages and **I** represents phase currents measured at PCC. **E** stands for equivalent voltage source and **Z** for complex line impedance. **V**, **I**, **E** ∈ ℂ and are presented in dq synchronous reference frame. **Z** ∈ ℂ and is expressed in (57).

$$\mathbf{Z} = \mathrm{R_{eq}} + \mathrm{j}\omega\mathrm{L_{eq}} = \mathrm{R_{eq}} + \mathrm{jX_{eq}} \tag{57}$$

In [37] capacitance is decided to leave out from the grid model because long distribution lines situated in rural areas are associated with highly inductive and resistive behavior. It is stated that capacitance gains more importance in residential areas but e.g. power factor compensation is not referred. Principle of aligning of measurement points in different operation points is illustrated in figure 3.3. Operation point is determined by the P, Q combination of the inverter.

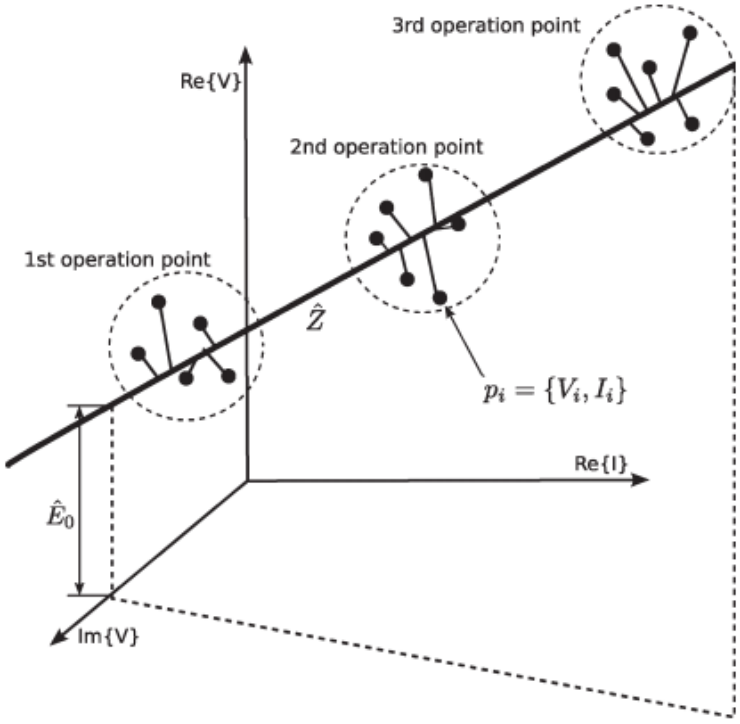

Figure 3.3. *Principle of estimating impedance with linear regression.[37, p. 3]*

With n different measurement points a set of linear equations (58) can be build.

$$\begin{cases} \mathbf{V}_0 = \mathbf{I}_0 \cdot \mathbf{Z}_0 + \mathbf{E}_0 \\ \mathbf{V}_1 = \mathbf{I}_1 \cdot \mathbf{Z}_1 + \mathbf{E}_1 \\ \vdots \\ \mathbf{V}_{n-1} = \mathbf{I}_{n-1} \cdot \mathbf{Z}_{n-1} + \mathbf{E}_{n-1} \end{cases} \tag{58}$$

When grid is stationary it can be quite accurately assumed that $\boldsymbol{E}_0 = \boldsymbol{E}_1 = \boldsymbol{E}_{n-1}$ and $\boldsymbol{Z}_0 = \boldsymbol{Z}_1 = \boldsymbol{Z}_{n-1}$. (58) can be expressed in matrix form (59) where $\boldsymbol{B} \in \mathbb{C}^{nx1}$, $\boldsymbol{A} \in \mathbb{C}^{nx2}$ and $\boldsymbol{X} \in \mathbb{C}^{2x1}$.

$$\mathbf{B} = \mathbf{A} \cdot \hat{\mathrm{X}} \tag{59}$$

The structure of $\hat{\mathrm{X}}$, the parameter vector, **B** and **A** is presented in (60).

$$\boldsymbol{B} = \begin{pmatrix} \boldsymbol{V}_0 \\ \boldsymbol{V}_1 \\ \vdots \\ \boldsymbol{V}_{n-1} \end{pmatrix},\ \boldsymbol{A} = \begin{pmatrix} \boldsymbol{I}_0 & 1 \\ \boldsymbol{I}_1 & 1 \\ \vdots & \vdots \\ \boldsymbol{I}_{n-1} & 1 \end{pmatrix},\ \hat{\mathrm{X}} = \begin{pmatrix} \boldsymbol{Z} \\ \boldsymbol{E}_0 \end{pmatrix} \tag{60}$$

Determination of impedance is a linear regression problem in complex field as presented in figure 3.3. The algorithm produces measurement points which cluster around an operation point. Deviation of measurements is caused by noise and small variations in operation point. In order to form estimation of grid equivalent impedance and voltage source the algorithm needs measurement points from at least two operation points. [37]

If an estimated parameter vector $\hat{\mathrm{X}} = \left(\hat{\mathrm{Z}}\ \hat{\mathrm{E}}_0\right)^{\mathrm{T}} \in \mathbb{C}^{2\mathrm{x}1}$ is assumed the matrix expression in (61) can be written.

$$\mathbf{B} = \mathbf{A} \cdot \hat{\mathrm{X}} - \mathbf{Q} \tag{61}$$

In (61) $\mathbf{Q} \in \mathbb{C}^{\mathrm{nx}1}$ is a vector for error between estimated voltage value calculated from the product between **A** and $\hat{\mathrm{X}}$ and actual measured output voltage. Best-fit for the parameter vector $\hat{X}$ can be found by minimizing error function. Error function minimization process is described in detail in [38]. It is shown in [38] that the optimal parameter vector will be as described in (62).

$$\hat{\mathrm{X}} = (\mathbf{A}^{\mathbf{T}} \cdot \mathbf{A})^{-\mathbf{1}}(\mathbf{A}^{\mathbf{T}} \cdot \mathbf{B}) \tag{62}$$

However, development of (62) is an offline procedure and is not valid for the purposes of this algorithm. To transform (62) into recursive algorithm a set of matrices from (63) and (64) leading to (65) are considered.

$$\boldsymbol{P}_k = ([\boldsymbol{A}^{T*}]_k[\boldsymbol{A}]_k)^{-1} \tag{63}$$

$$\boldsymbol{C} = \begin{pmatrix} \boldsymbol{I}^*_{k+1} \\ 1 \end{pmatrix} \tag{64}$$

$$\boldsymbol{D_{k+1}} = \boldsymbol{P}_{k+1}\boldsymbol{C} \tag{65}$$

It can be demonstrated that (66) gives a straight forward way of estimating grid equivalent voltage source and impedance. [38, pp. 2-4]

$$\begin{pmatrix} \hat{\mathrm{Z}} \\ \hat{\mathrm{E}}_{\mathbf{0}} \end{pmatrix}_{\mathbf{k+1}} = \begin{pmatrix} \hat{\mathrm{Z}} \\ \hat{\mathrm{E}}_0 \end{pmatrix}_{\mathbf{k}} + \mathbf{D}_{\mathrm{k+1}} \cdot \mathrm{q}_{\mathrm{k+1}} \tag{66}$$

The effectiveness and accuracy of this algorithm is straightly proportional to the Euclidian distance separating the operation points in which the measurements are taken. In [37] an evaluation subsystem is presented. The core idea is to monitor a windowed error variable Γ_{k} presented in equation (67).

$$\Gamma_{\mathrm{k}} = \frac{1}{2\mathrm{k}} \sum_{\mathrm{i=k-n}}^{\mathrm{k+n}} \frac{\left\|\mathbf{V_i} - \mathbf{I_i}\hat{\mathbf{Z}}_{\mathrm{i}} - \hat{\mathbf{E}}_{\mathrm{i}}\right\|^2}{|\mathbf{I_i}|} \tag{67}$$

The estimation process begins in idle state during which the system samples measurements in zero current operation point. After the converter starts producing active and reactive power to the grid the algorithm will have the minimum of two operation points to start the estimation process. This, the regular operation, state will remain as long as the error variable remains below predetermined threshold. After the error variable exceeds its threshold the algorithm will reset and start sampling a new operation point. Resetting is done to speed up the algorithm's convergence towards new grid equivalent

parameters. To gather measurements from two required operation points the system then moves to a grid perturbation state until the error variable falls below the threshold. This gives this algorithm its hybrid nature as an islanding detection method. The algorithm can be operated without the windowed error variable and grid perturbation state but this will affect significantly the accuracy especially with high power applications. After the condition with error variable is fulfilled, new values for grid equivalent voltage source and impedance will be considered valid and they can be compared with predetermined thresholds for islanding detection. Finding the threshold for grid equivalent impedance and voltage source from which islanding is concluded or error variable value at which the algorithm moves into grid perturbation state has to be done carefully. Different grid conditions in which the inverter can operate have to be determined. Possibly the thresholds for islanding detection have to be dependent on the grid configuration to minimize the possibility of false detection. [37, p. 5]

3.5 Applicability of islanding detection methods

Applicability into different kinds of DG and effectiveness of presented methods is discussed in this chapter.

Passive islanding detection methods are based on monitoring voltage or current at inverter terminal or PCC. Passive detection is most common method of islanding prevention and minimum requirement for any DG unit. Traditionally high power applications are equipped with external protection relays taking care also of islanding protection but implementation of passive methods into DG is rather easy and does not consume much computing resources. Simplest passive islanding detection method is the use of frequency and voltage windows. Relation of voltage and active power and that of frequency and reactive power is straight forward when it comes to power systems consisting only inverter operated generation. When there is synchronous machines connected within the system the relation is more complicated and is mainly determined by excitation and governor control of the machines. In a system where there is a possibility that generation and production within an islanded system is closely matched, frequency and voltage windows are not considered sufficient for islanding detection.

Voltage harmonic, voltage unbalance and phase monitoring methods can in some cases be effective indicators for islanding but it depends strongly on the configuration of the islanded power system and finding thresholds for reliable detection is difficult. Inverter –, especially high power, applications create harmonic distortion themselves which can make conclusions based on THD difficult to obtain. Effectiveness of voltage unbalance and phase monitoring is solely dependent on loading of the islanded system. If the islanded grid is symmetrical and reactive power is balanced islanding detection will fail.

Rate of change of frequency and rate of change of frequency over power are mostly suitable for power systems where islanded system will in addition to inverters contain also synchronous machines. However, they are most effective of the presented passive

methods and don't require additional measuring and consume little computational capacity. Thus, they would be easy and cost effective to implement into an inverter unit. The passive nature of these methods, however, results in that these methods do have an NDZ and the possibility of nuisance tripping because of e.g. load changes is apparent.

Various impedance estimation methods has been suggested from which two active islanding detection methods, characteristic and non-characteristic harmonic injection, are considered in this thesis. Characteristic harmonic injection consumes lot of computing capacity and thus, is difficult to be implemented into a DG inverter. Non-characteristic harmonic injection doesn't require as much processing power but still there is a need for DFT calculation. All harmonic injection effectively decreases the power quality of the DG unit by increasing THD. However, non-characteristic harmonic injection has yielded to quite accurate results in impedance estimation and reliable islanding detection in tests conducted in [24]. Applicability on weaker grids, in grids where impedance changes occur naturally and the possibility that linearity assumption of the impedance is not valid are weak points of this method.

Active – and reactive power variation methods' effectiveness depends on the grid configuration, i.e. if there are synchronous machines controlling voltage level and frequency within the power system. Active power variation methods are not very effective because variation needed to carry the voltage out of acceptable range is quite substantial and results in e.g. flickering. Islanding detection based solely on voltage level is very difficult because of wide voltage ranges DGs are required to operate in. Sandia voltage shift also uses active power variation to inflict changes in voltage amplitude by variation in current amplitude and tries to overcome problems with wide voltage range by monitoring the response in voltage rather than absolute level of it. However, SVS is not considered very effective to be used alone. Reactive power variation with positive feedback from frequency error with only inverter based DG supplying the islanded power system has a relatively small NDZ but when there is synchronous machines present maintaining frequency and capable of sinking or supplying the reactive power produced by the inverter the islanding detection is more difficult. This method also has a natural NDZ, if there is no frequency error to start with islanding cannot be detected. However, reactive power variation has a small effect during normal operation and it easy to implement in inverter control.

Different variations of active frequency drift methods are based on introducing a dead time in inverter output current resulting in phase shift between the fundamental component of the output current and grid voltage which will in an islanding situation carry the frequency to a trip limit. All of the AFD methods introduce an increase in THD level and they are not suited for applications in which unity power factor control or grid voltage support is required. This excludes them from most DG applications. However, AFD methods can be very effective in islanding detection.

Slip mode frequency shift and automatic phase shift are based on deviation of the inverter output current starting angle on basis of frequency error. Intention is to carry the system frequency to trip limit when islanding occurs. As AFD also these methods

introduce a phase shift between inverter current and grid voltage during normal operation and thus are not suited for most DG applications. To overcome these problems a method called adaptive logic phase shift which uses measured frequency rather than nominal frequency when calculating frequency error is developed. ALPS minimizes effects of islanding detection functionality during normal operation, it does not require much computing resources and is rather easy to implement into a DG inverter.

Hybrid islanding detection methods are most suitable for modern power quality requirements and they offer effective islanding detection. Various hybrid methods have been developed from which three are introduced in this thesis. Most suitable one for DG inverter implementation is covariance of current and voltage periods and adaptive reactive power shift. Voltage unbalance monitoring based frequency set point variation is not very effective since the probability that voltage unbalance is not high enough during islanding is rather high. Grid impedance estimation might be effective but calculations required are rather heavy and it requires quite accurate measurements to be effective. Covariance of voltage and current periods does not require heavy calculations if accurate enough measurements are available and as a passive method it does not have an effect on any inverter functionality during normal operation. ARPS to be applied when islanding is suspected also doesn't have drastic effects on power system even if the suspected islanding is not true. Downsides of ARPS are the same as with reactive power shift, if there are synchronous machines maintaining frequency and voltage reactive power injection does not have an effect on system frequency.

Many of the proposed islanding detection methods require too much computing resources when implementation into a DG inverter is at issue. Also, requirements for measuring accuracy are in many cases out of the scope of regular equipment within a DG inverter. Islanding detection is always a compromise between detection effectiveness and power quality.

4 ISLANDING TESTING

In this chapter the principles of islanding testing and regulations for distributed generations considering islanding are studied. Islanding is tested with and without the anti-islanding function. Testing is based on principles presented in IEEE 1547.1 [17] but also European standardization is referred. Testing without anti-islanding function is done to gather information on the behavior of the AFE control in islanding situation but also to be able to compare the results with and without anti-islanding functionality. This is important since currently there is no anti-islanding functionality implemented in existing products.

4.1 Anti-islanding function

Islanding detection technique under testing is based on positive feedback from frequency error to reactive current control which is referred to in chapter 3.3.4. Continuation of operation in islanded mode is difficult with this method since it will force the frequency out of permissible range for operation. Therefore this method can be referred to as an anti-islanding – rather than islanding detection method. Figure 4.1 presents the basic principle of anti-islanding and reactive current controllers. Effect of reactive current injection depends on the grid configuration of the islanded system. If there are synchronous machines controlling frequency, reactive current effects voltage levels of the system and if there are only inverters reactive current effects system frequency.

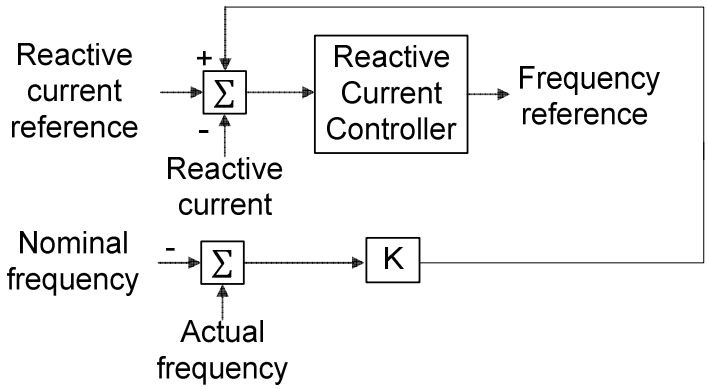

Figure 4.1 *Principle of the structure of tested anti-islanding - and reactive current controllers.*

Anti-islanding controller is a P-type controller which operates in parallel with reactive current controller. In Figure 4.1 the lower control branch which operates on the difference of grid nominal frequency and actual frequency at the converter terminal, i.e. fre-

quency error, is the anti-islanding controller. There is also available a gain parameter for the positive feedback loop of the anti-islanding controller presented by K. Reactive current controller consists of PI controller and PD controller which provides the frequency reference by derivation of the output of PI controller. Frequency reference is fed to modulator. Both controllers operate on same principles whether in islanding situation or not. The anti-islanding feature is enabled by setting a bit in firmware interface which is done with a parameter in application software. [12, pp. 9-10]

4.2 Grid regulations concerning islanding

Islanding in general is an old concern but for distributed generation operators and inverter manufacturers it is rather new issue and grid regulations concerning them has been developed quite recently. In addition to testing of islanding detection, regulations for e.g. permissible frequency and voltage ranges have an effect on islanding detection efficiency. Frequency range is especially important with anti-islanding methods operating on system frequency since it is proportional to tripping time of the DG unit.

Frequency range for a grid connected production unit slightly varies around the world. From islanding point of view it is the widest referred frequency range which should be considered since that will determine the limits for DG unit tripping in case of over – or under frequency. Within Scandinavia frequency range has been 47,5-53,0Hz and in ENTSO-E pilot code Nordic suggestion is for 47,5-52,5Hz. In ENTSO-E pilot code for continental Europe frequency range is wider 46,5-53Hz. There have been discussions especially in Germany on how strict frequency limits for solar inverters may cause problems in power system disturbances when a small deviation in frequency leads to a large portion of production to disconnect and make the situation more critical. Current regulations for wind turbines in Germany state a frequency window of 47,5-51,5Hz. There are slight deviations within European regulations but the target is to uniform European regulations with ENTSO-E. In united states permitted frequency range for DG smaller than 30kW is 59,3-60,5Hz and for above 30kW units 57,0-60,5Hz. [64, p. 35; 29, p. 9] Chinese requirements for wind farm operating frequency are not stating unambiguous limits at which the inverter should trip, thus currently excluding islanding detection based on frequency. However, Chinese development in grid regulations is often following Europe and in the future it is likely that considerations for islanding will be included in regulations. [39, p. 36]

For permissible operation ranges of voltage also grid fault situations affect the islanding detection. ENTSO-E pilot code Nordic states permissible voltage range from 90% to 110% of nominal voltage and ENTSO-E pilot code for continental Europe from 80% to 115%. Current regulations in Europe are inside these limits. In USA operation inside 88%-110% range is permitted. When considering islanding detection it should be noted that requirements for fault ride through capabilities require DG units to stay grid connected for short times even with zero grid voltage. This functionality introduces significant delays into islanding detection or even excludes voltage level monitoring as an

islanding detection method. Also, fault ride through functionality might have an effect on frequency based islanding detection since it is possible that the grid inverter will freeze its frequency during very low impedance faults to a pre-fault value. [40, p. 38; 29, p. 8]

All grid codes do not consider requirements for islanding very precisely. In Europe the basic requirement for islanding detection is a protection relay for under – or over frequency and under – or over voltage. German grid code requires also grid impedance measurement for units rated under 30kW. Grid impedance measurement is forbidden in UK but a ROCOF-based protection is required. ENTSO-E does not have requirements for islanding prevention but it is mentioned that a DG unit should be able to stay grid connected in an island constituting a suitable amount of production and consumption. Usually issues related to islanding are dealt with in distribution grid requirements. [40, p. 84] In [29] it is stated that DG unit shall detect and cease to energize an island in less than two seconds. Means by which this is achieved are mentioned to be e.g. DG capacity limitation to less than one third of the minimum load of possible island, a transfer trip signal or a tested anti-islanding functionality. [29, p. 10]

In this thesis the objective of miniature testing is to gather information of the available islanding detection method rather than aim at certification or full compatibility with standardization. The setup is build with minimum costs and thus is not in full compliance with standardization. If it is wanted to review the results of islanding detection testing from the perspective of grid codes it has to be done separately. In these tests a frequency window of +/-2,5Hz is adopted from European standardization [40]. Acceptable tripping time of two seconds and principle of the test setup and test procedure has been adopted from IEEE standardization but test procedures are fairly similar also in Europe. [17, 29]

4.3 Miniature setup for islanding testing

Electric circuit diagram of the test setup is presented in appendix 1. The setup consists of a 12A AFE fed by 12A rectifying inverter and permanent magnet synchronous generator. Generator is rotated by an induction machine. Islanding load consists of a parallel RLC circuit. Islanding of the setup is done with a manual switch which disconnects the setup from the grid. The principle by which the AFE is fed to the DC bus does not play a significant role and can represent a wide range of primary energy sources, e.g. wind – or solar energy. The setup nominal voltage is 400V.

4.3.1 Back-ground behind the testing environment

The reason for introduction of resonance circuit is to have a stabilizing element to the islanding circuit which results in more difficult conditions for islanding detection. In real power systems stabilizing elements are introduced by rotating machines and generators of the system in addition to reactive power stored in system’s inductances and capacitances. In some islanding studies also rotating machines have been connected to

test setups. It is evident that rotating machine does have a physically different effect on the islanding circuit but it is comparable with a resonant circuit since both of them increase the probability to maintain grid frequency once islanding has occurred. Because the reproducibility of an islanding test setup containing also rotating machine would require the machine properties such as inertia and friction as well as active – and reactive power control systems to be standardized, the resonant circuit with rather high quality factor is adopted as a sole stabilizing element in Europe, USA and Australia. [41, p. 3]

Whether the resonant circuit reactive power should have an absolute value rather than a specified quality factor has also been discussed. An absolute value for reactive power would result in more difficult islanding conditions for smaller inverters and partial load conditions. Standardization of a specified quality factor rather than absolute amount of reactive power is useful since it offers scalability to the test setup. In USA a quality factor of 2,5 was required in [18] until 2006. Reasoning behind this is that a quality factor of $Q_f \leq 2{,}5$ equates to distribution lines with uncorrected power factors from 0,37 to unity but moreover it represents stabilizing elements such as synchronous machines within the power system. When a worst case scenario in which the reactive supply exactly matches reactive load is assumed the power factor can be mathematically associated with power factor as in equation (65). [18]

$$\mathrm{Q_f} = \tan\left(\arccos\left(\mathrm{PF}\right)\right) \tag{65}$$

In [17] which has replaced [18] the requirement for quality factor is one which equates to power factor 0,707. It is stated that power systems typically operate above power factor 0,75 under steady-state conditions and therefore the quality factor of one is below the power factor the distributed resource is expected to island with. Also a lower value of Q_f allows inverter manufacturers to use active islanding detection methods in which the perturbations for power system are less harmful. In UK it is proposed to have a quality factor of 0,5. Reasoning behind this is that quality factor of 0,5 is thought to represent another inverter connected to the grid section to increase the probability of the grid to maintain its nominal frequency when in islanding situation. In IEC 62116 draft B4 a Q_f of 0,65 is used. [17]

4.3.2 Measurement equipment

Measuring and recording of system quantities is done with Elspec blackbox 4500G. Phase voltages are connected straight to blackbox and currents are measured with Fluke i1000s current probes. Accuracies of the used equipment are presented in table 4.1.

Table 4.1. *Accuracies of measurement equipment.*

	Voltage	Current	Frequency
Accuracy	0,1 %	3,0 %	10mHz
Sampling rate	1024 /cycle	256 /cycle	1024 / cycle

In addition to uncertainties related to measuring of system quantities the sampling rate of digital measuring device affects the measurement. In [17] it is stated that the minimum accuracies of the measurement equipment for voltage and current shall be 1% or less of the rated output quantity of the equipment under testing. For Fluke i1000s this requirement is not met above four amperes operating points as the accuracy of the current probe is 3% of the reading when using measurement range of 100mV/A. Accuracy of the measured quantity can be calculated as in equation (66).

$$\eta_{\mathrm{tot}} = \frac{\eta_{\mathrm{me}} \cdot \mathrm{reading}}{\mathrm{nom.quantity}} = \frac{3\% \cdot 4\mathrm{A}}{12\mathrm{A}} = 1\% \tag{66}$$

Equation (66) shows the relativity of the current probe accuracy in relation to operating point and nominal value of the measured quantity. In (66) η stands for accuracy and sub clauses *me* for measurement equipment and *tot* for total. During and in subsequent to islanding the current flowing at PCC to or from the grid is always smaller than four amperes from which it follows that the measurement accuracy is within the limits stated in [17]. For sampling frequency it is stated that it should be appropriate for measuring the fundamental frequency component. The sampling frequencies of 256 samples per cycle for current and 1024 samples per cycle for voltage yield to absolute sampling frequencies of 12,8kHz and 51,2kHz, respectively. It can be stated that these values are within the appropriate values meant in [17].

4.3.3 Islanding load

The islanding load is a parallel RLC load and three phase diagram of the load is presented in appendix 1. The LC circuit is tuned to have resonance at the grid frequency. This is utilized with an inductance of three times $33{,}7mH$ connected in Y and a capacitance of three times $99\mu F$ connected in Δ. One $99\mu F$ capacitor branch constitutes of $68\mu F$, $22\mu F$ and $9\mu F$ capacitors. Connections of the LC circuit are designed in order to minimize costs of the setup. A Δ-connected capacitance is transferred to equivalent Y-connected capacitance by multiplying by three as in equation (67). Resonant frequency of an LC circuit is calculated as in equation (68).

$$\mathrm{C_Y} = 3\mathrm{C_\Delta} = 3 \cdot 99\mu\mathrm{F} = 297\mu\mathrm{F} \tag{67}$$

$$\mathrm{f_R} = \frac{1}{2\pi}\sqrt{\frac{1}{\mathrm{LC}}} = \frac{1}{2\pi}\sqrt{\frac{1}{297\mu\mathrm{F} \cdot 33{,}7\mathrm{mH}}} = 50{,}3\mathrm{Hz} \tag{68}$$

In (67) and (68), L and C stand for load inductance and capacitance, and f_R stands for resonant frequency. The tolerance of the capacitors is +/-10% and the tolerance of the inductors is -5% / +10%. In worst case this would result in the resonant frequency varying from $45{,}7Hz$ when both L and C are 10% over the specified and $54{,}4Hz$ when C is 10% smaller and L is 5% smaller than specified. Thus, the accuracy of sizing resulting in $50{,}3Hz$ can be considered acceptable. According to [29] the testing is to be started with LC resonance at grid frequency and then continued with L or C diverged from that value with 1% steps in a range of +/-5%. In this setup diverging is done by tapping the phase coils of the inductance.

These inductance and capacitance values will result in 15kVAr of reactive power fed and consumed within the islanding load. Resistance of the setup is 26Ω connected in Y which results in 6kW of active power consumption. This relation of reactive and active power yields to a quality factor, Q_f, of 2,5 as presented in equation (70). Equation (69) applies for a parallel RLC load in general and (70) for a grid frequency resonant parallel RLC circuit. In (70) it is assumed that active – and reactive powers do not depend on each other, i.e. reactive power level does not affect voltage.

$$Q_f = R\sqrt{\frac{C}{L}} \tag{69}$$

$$Q_f = \frac{Q}{P} = \frac{15kVAr}{6kW} = 2{,}5 \tag{70}$$

In (69) and (70) R stands for resistance and Q and P represent reactive – and active power. Q_f can be mathematically associated with power factor of the islanded section of the power system as in equation (65). The selected Q_f of 2,5 would result in an uncorrected power factor of 0,37. Calculation of PF from active and reactive power is presented in (71).

$$\mathrm{PF} = \frac{\mathrm{P}}{\mathrm{S}} = \frac{6\mathrm{kW}}{\sqrt{(6\mathrm{kW})^2+(15\mathrm{kVAr})^2}} = 0{,}37 \tag{71}$$

When the effect of AFE's LCL filter is taken into account the quality factor cannot be calculated as it would be in grid resonant case. LCL inductances are in series and valued 4,1mH and 8,1mH. Capacitance is 2,2µF in parallel and connected in Δ. When the effects of LCL filter are taken into account Q_f can be calculated with equation (69). When $C_Y = 3\ C_\Delta$ and parallel capacitances can be summed resulting in total capacitance of 303,6µF. When superposition theorem is applied and AFE is thought as a current source, inductances of the setup are in series and can be summed as well resulting in total inductance of 45,9mH. This yields to a quality factor of 2,11 as calculated in (72).

$$Q_f = 26\Omega\sqrt{\frac{303{,}6\mu\mathrm{F}}{45{,}9\mathrm{mH}}} = 2{,}11 \tag{72}$$

Regardless of the offset in reactive power introduced by LCL and any non-idealities within the setup and testing environment, the reactive power fed to – or taken from the grid can be tuned to zero by adjusting the reactive power of the AFE. As the AFE will compensate its LCL filter in any case this does not have an effect on the principle of the islanding detection testing. Also in real power systems AFE's can also be consuming or producing reactive power for reactive loads of the power system or supporting the grid voltage with reactive current during steady state operation.

The islanding load as it is built is presented in figure 4.2. In figure 4.2 parts of the islanded load, resistance, inductance and capacitance are marked with numbers one, two and three, respectively. Tapping points of the inductor are seen on top of each phase coil. Numbers six in figure 4.2 mark the manual switches for connecting each part of the load to the circuit. Number four marks the point of common coupling of the load, utility grid and AFE. PCC is also the point where currents and voltages are measured. Number five marks the circuit breaker for the whole RLC load capable of disconnecting circuit

in case of short circuit. Breaker can also be operated as a manual switch. Number seven marks the point where the resistance is connected.

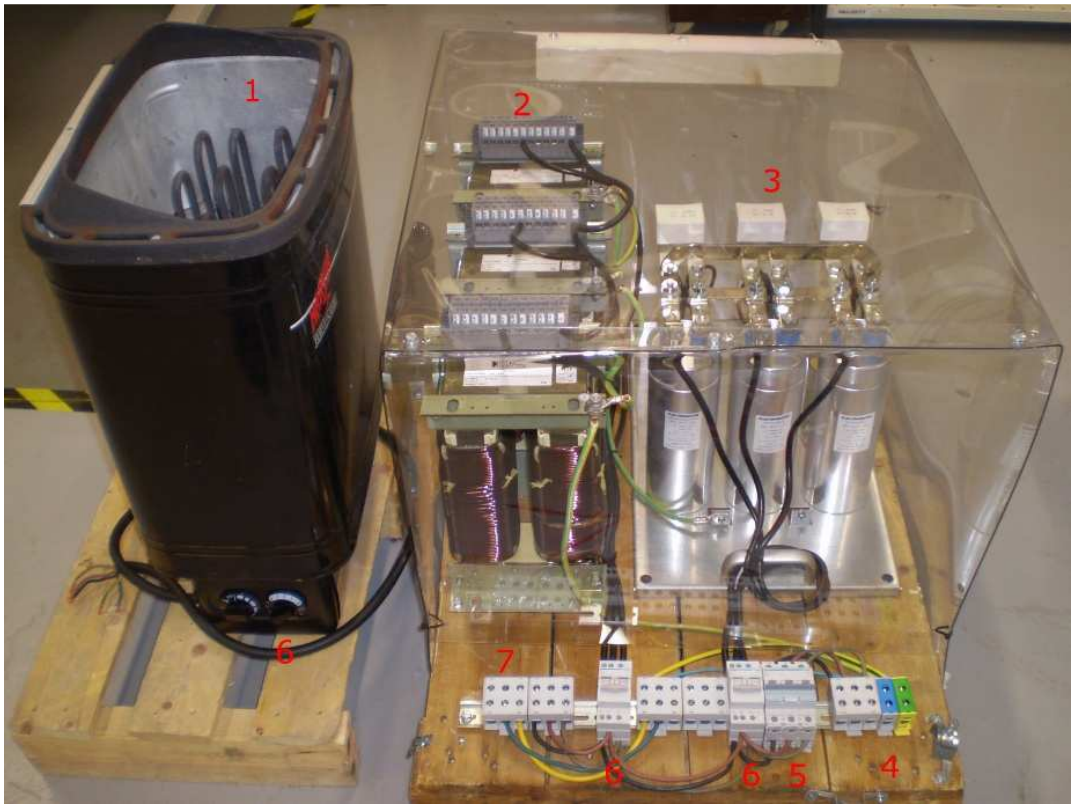

Figure 4.2. *Parallel RLC load for islanding testing.*

4.4 Initial conditions for islanding

Principle for the test procedure and achieving initial conditions for islanding of a non-islanding inverter is adapted from [17]. The initial conditions in which the testing is to be done are achieved by adjusting the active – and reactive power production of the AFE so that the current flowing between the grid and test setup is minimized. Fundamental components of currents and powers need to be used when tuning the initial conditions because of the high amount of harmonic content.

In figure 4.3 the phase reactive power at fundamental frequency and main voltages at PCC when only passive RLC load is energized are presented. Referring to circuit diagram of appendix 1, breakers BR1 and BR2 are closed while BR3 remains open. Switches SW1-3 are closed. Reactive power is examined in order to verify that L and C of the test setup are compensating each other, i.e. LC circuit is resonating at 50,3Hz as calculated in (68). There is a step change at the point of 2000ms where resistances are disconnected and only L and C remain energized. In circuit diagram of appendix 1 switch SW1 is opened while switches and breakers remain at their previous states. It is evident that resistances have also reactive properties which are relatively highly unsymmetrical because the disconnection of them is seen as an unsymmetrical change in reactive powers.

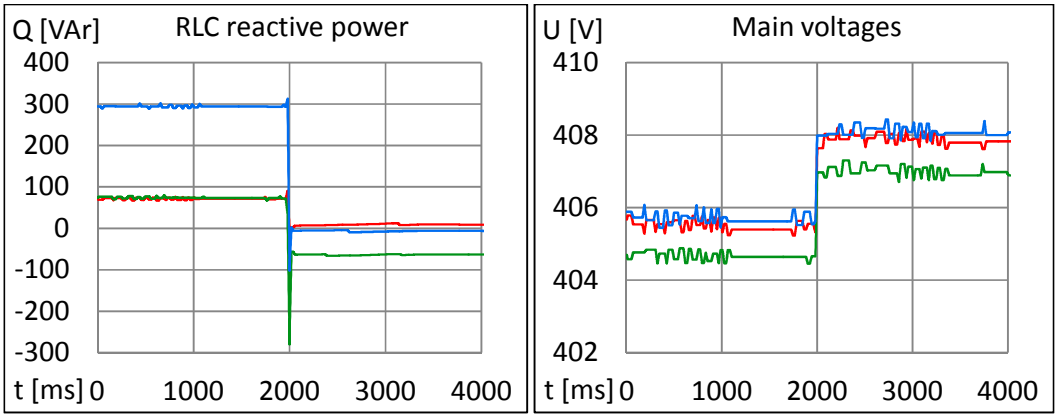

Figure 4.3. *Reactive power and main voltages of the RLC load. Red color indicates L1 reactive power and L1-to-L2 voltage, green indicates L2 reactive power and L2-to-L3 voltage and blue indicates L3 reactive power and L3-to-L1 voltage.*

Asymmetry in main voltages explains also the asymmetry in phase reactive powers when only LC load is connected after 2000ms in figure 4.3. The disconnection of the resistance also affects the main voltages because the voltage drop over cables and connectors all the way from the main transformer is current dependent. Reactive power shift towards capacitive, i.e. negative, in all phases at the disconnection of resistances is explained by in-series inductive elements, namely inductance of cables and connectors, of the setup and symmetrical reactive properties of resistances. These elements generate a small amount of inductive power which is dependent on the current flowing through them.

In figure 4.4 RMS values of fundamental, 50Hz component of current and total RMS current are presented when only load inductance and capacitance are connected to grid. In circuit diagram of appendix 1 breakers and switches remain at their previous states. At the point of 2000ms the AFE of the frequency converter which is rotating the induction machine starts modulation. It is evident that the fundamental component needs to be used in order to adjust the reactive - and active power balances within the setup as it is recommended in [17] because of the total RMS current rising as high as

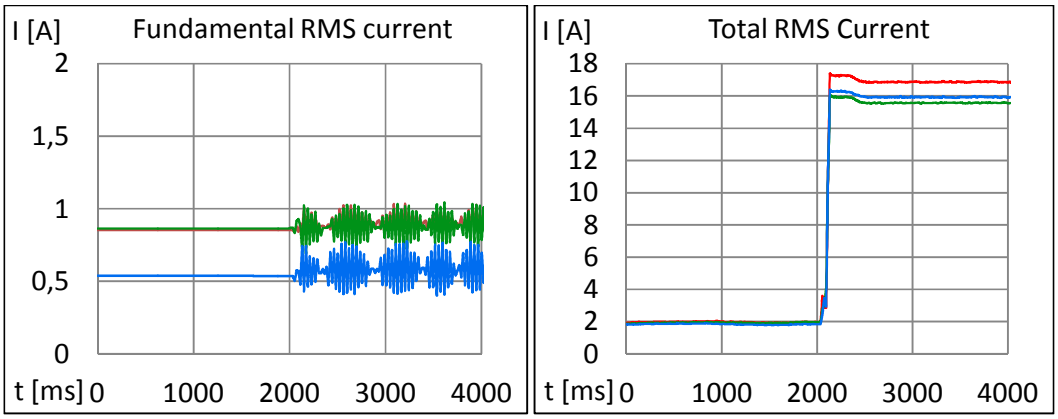

Figure 4.4. *RMS values of islanding setup's fundamental and total phase currents when only LC is connected. Red color indicates L1, green L2 and blue L3 current.*

17A due to harmonic components inherent from the PWM of the rotating AFE. High harmonic content is seen also as ripple in the fundamental RMS current.

The harmonic content of the current when only passive LC load is connected and rotating AFE is modulating is presented in figure 4.5. Clearly dominant components are centered around 60th harmonic component which is inherent from 3,0kHz switching frequency of the rotating AFE. The fact that the sidebands, 58th and 62nd component are dominant rather than the 60th is inherent from the used modulation technique. Other elevated frequencies in the current are 7th, 11th, 13th and 17th component. These are inherent from AFEs six-pulse switching. The spectrum in figure 4.5 is limited to first 80 components but it is noted that also sidebands of multiples of the 60th harmonic, i.e. 120th and 180th are visible in the current spectrum.

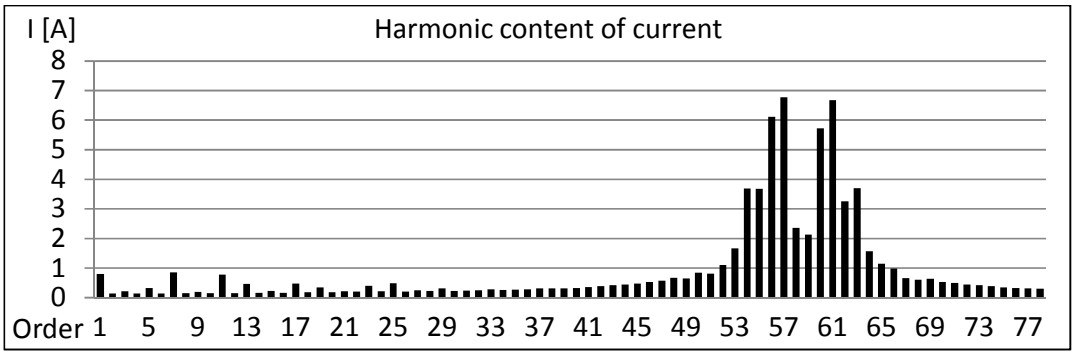

Figure 4.5. *Spectrum of the current when rotating AFE is modulating and LC is connected to the grid.*

It is recommended in [17] that the current flowing through the PCC when consumption and loading of active - and reactive power is matched should be less than 2% of the nominal current of the inverter under testing. In figure 4.6 the current has been adjusted as small as possible. Here all breakers BR1-3 and switches SW1-3 are closed and all inverters are running.

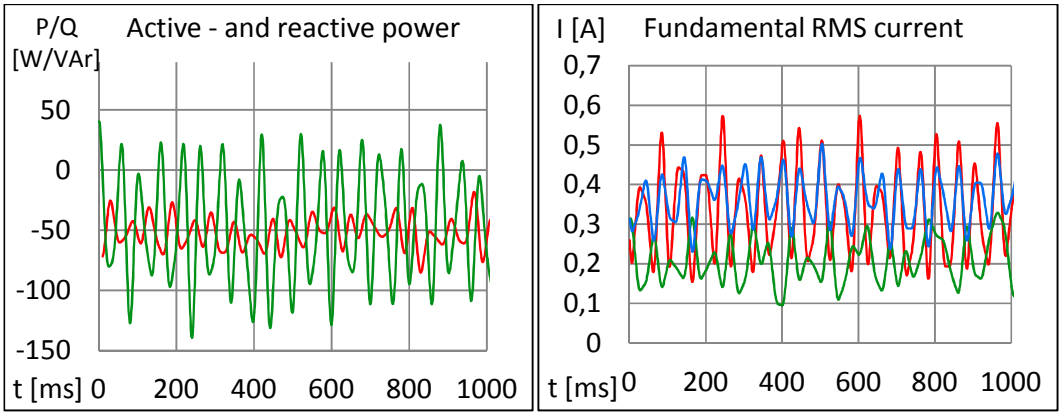

Figure 4.6. *Fundamental RMS currents at PCC with matched active – and reactive power within the islanding setup. On the left green indicates reactive power and red active power. On the right red indicates L1, green L2 and blue L3 current.*

It can be approximated that fundamental current component flowing through PCC is 0,3A by calculating the average of samples of all three phases' fundamental current components. Smaller value could not be achieved because of variations in PQ operating point caused by heating of mainly resistance of the load but also reactive components and supplying generator as well as small variations in grid voltage level. 0,3A is 2,5% of the nominal current of 12A and this is above the requirement of 2%. In figure 4.6 the frequency of oscillation in currents and powers is at approximately 19Hz. Oscillations could be due to time constants of the AFEs' current controllers. Negative values of the powers in figure 4.6 indicate that active power is flowing from the AFE to the grid and reactive power is capacitive. Apparent power can be calculated as in equation (73).

$$S = \sqrt{P^2 + Q^2} = \sqrt{(50W)^2 + (50VAr)^2} = 70VA \quad (73)$$

Tuning the initial conditions in this test environment proved very challenging because of high amount of harmonic content and asymmetry within the setup. Also there is drifting in the operation point of the setup due to heating of the resistances and other components which affects the value of resistance and therefore current, but also reactive elements.

4.5 Islanding without anti-islanding functionality

In figure 4.7 islanding happens at the point of 1000 milliseconds. Before islanding all breakers and switches are closed in circuit diagram of appendix 1 and islanding is realized by opening breaker BR1. Initial settings found for the converter under testing in previous chapter are kept constant throughout the whole test procedure. Only the load inductance is varied and anti-islanding function is set on or off. Frequency of the system finds its steady state value immediately and remains at nominal 50Hz. Ripple in the frequency before islanding is inherent from the current ripple of the rotating AFE and it is cleared after islanding.

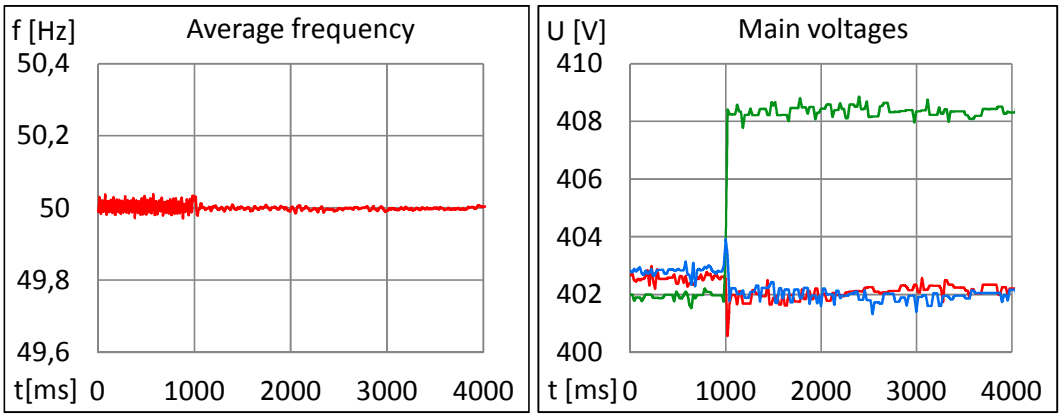

Figure 4.7. *Average system frequency and main voltages of the test setup in islanding situation without anti-islanding function and matched PQ-balance. Red color indicates frequency and L1-to-L2 voltage, green indicates L2-to-L3 voltage and blue indicates L3-to-L1 voltage.*

Reason for high amount of harmonic content introduced by rotating AFE is that it is significantly bigger unit than inverters under testing. Average frequency of the system is calculated from individual phase frequencies. In figure 4.7 both frequency and voltages are plotted with one millisecond sampling. Also main voltages of the setup remain within acceptable values after islanding. Main voltages L1-to-L2 and L3-to-L1 remain close to their pre-islanding values but L2-to-L3 steps up about six volts. This asymmetry in voltages after islanding is inherent from the asymmetry of the resistive components in the islanding load and tendency of the AFE to respond to asymmetrical voltages with asymmetrical current.

If the inductance of the islanding load is diverged by +/-1% the resulting frequency and main voltages are presented in figures 4.8 and 4.9. Resonant frequencies with inductance values 33,4mH and 34,0mH are calculated in (74) and (75), respectively.

$$f_R = \frac{1}{2\pi}\sqrt{\frac{1}{297\mu F \cdot 33{,}4mH}} = 50{,}6Hz \quad (74)$$

$$f_R = \frac{1}{2\pi}\sqrt{\frac{1}{297\mu F \cdot 34{,}0mH}} = 50{,}1Hz \quad (75)$$

The trend indicated by calculation of the resonant frequencies is visible in measured frequencies but actual values in steady state are more dependent on the overall reactive balance of the setup. From figure 4.8 it is seen that when the islanding load is diverged towards capacitive the frequency shifts upwards.

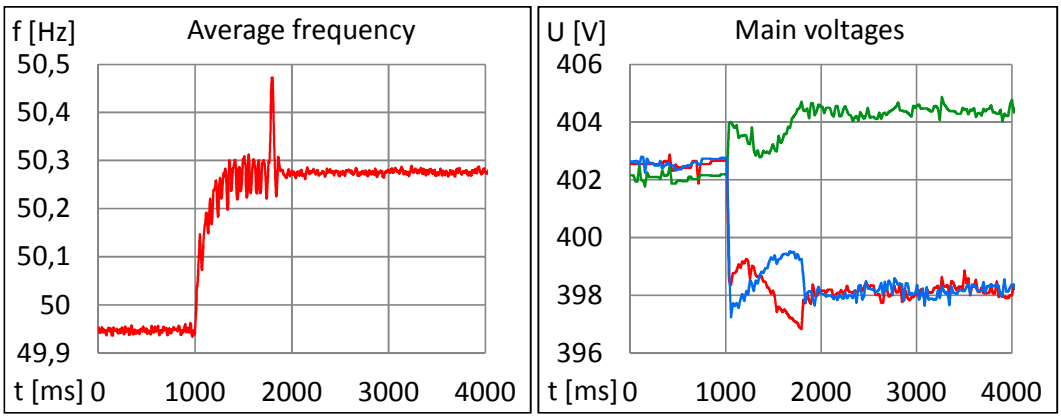

Figure 4.8. *Average system frequency and main voltages of the test setup in islanding situation without anti-islanding function and load inductance of 33,4mH. Red color indicates frequency and L1-to-L2 voltage, green indicates L2-to-L3 voltage and blue indicates L3-to-L1 voltage.*

Shift towards capacitive loading is done by tapping the islanding load from 33,7mH to 33,4mH. This change in inductance decreases the inductive reactance which results in greater inductive power sank by the islanding load. This raise in inductive power within the island is then compensated by a raise in frequency. When frequency increases the capacitive reactance decreases. Smaller reactance results in more current and, thus, more capacitive power. Inductive – and capacitive reactances can be calculated as in equations (76) and (77).

$$X_C = \frac{1}{2\pi f C} \quad (76)$$

$$X_L = 2\pi f L \quad (77)$$

In (76) and (77) C and L stand for capacitance and inductance, respectively, and f stands for frequency. Reactive power for a three-phase system can be calculated with (78).

$$Q = 3I^2X = 3\frac{U^2}{X} \quad (78)$$

In equation (78) X stands for capacitive or inductive reactance, I and U stand for RMS current and RMS phase-voltage. [42]

The response to islanding in frequency and voltage when islanding load inductance is increased by 1% to 34,0mH is seen in figure 4.9. It is evident that responses are opposite to those when inductance is decreased, i.e. frequency decreases and voltage increases.

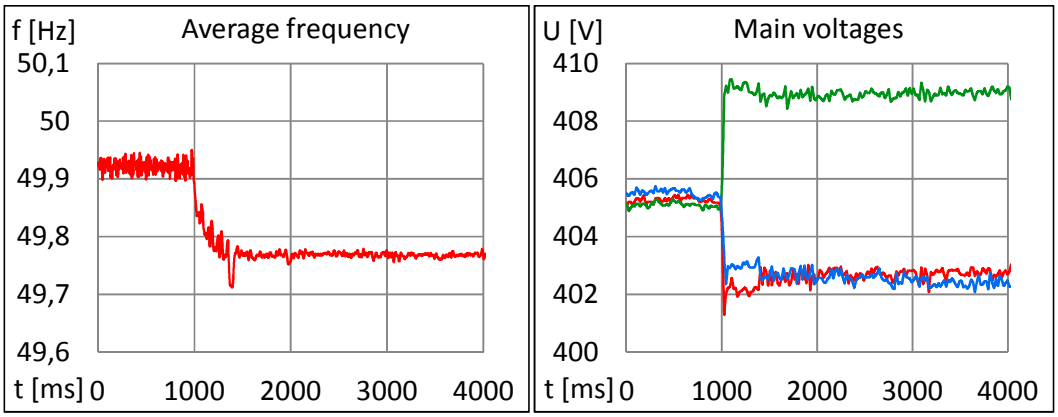

Figure 4.9. *Average system frequency and main voltages of the test setup in islanding situation without anti-islanding function and load inductance of 34mH. Red color indicates frequency and L1-to-L2 voltage, green indicates L2-to-L3 voltage and blue indicates L3-to-L1 voltage.*

The response in voltages with different load inductances should be similar. However, the difference in steady state voltage levels is 4-5V. This is explained by active power levels prior to islanding. In the situation of figure 4.8 there was approximately 110W and in the situation of figure 4.9, 25W fed from the grid to the islanding system. These are average values of 1ms samples during 1s before islanding. According calculatory voltage levels after islanding in the situations of figures 33,4mH and 34,0mH is calculated with equation (12) in (79) and (80), respectively.

$$\mathrm{U}'_{\mathrm{Isl}} = \sqrt{\frac{6{,}6\mathrm{kW} - 120\mathrm{W}}{6\mathrm{kW}}} \cdot 402{,}3\mathrm{V} = 398{,}6V \quad (79)$$

$$\mathrm{U}'_{\mathrm{Isl}} = \sqrt{\frac{6{,}6\mathrm{kW} - 20\mathrm{W}}{6\mathrm{kW}}} \cdot 405{,}3\mathrm{V} = 404{,}7\mathrm{V} \quad (80)$$

In (79) and (80) 6,6kW is power calculated from AFE's current measurements and voltage are average values of samples during 1s in prior to islanding. Despite the asymmetry of voltages, results of (79) and (80) are in compliance of the measured voltages in figures 4.8 and 4.9. Average of 1ms samples in the islanded system are 400,2V and

404,7V, respectively. Asymmetry of voltages is explained by asymmetry in the resistances of the islanding load. Steady state angular frequency after islanding when the reactive power balance is taken into account can be calculated with equation (14). Frequency is obtained by dividing angular frequency by 2π. Calculation with 33,4mH load inductance is done in (81) and with 34mH inductance in (82).

$$\omega' = \frac{1}{4\pi}\left[\frac{118\text{VAr}}{297\mu\text{F}\cdot(400{,}2\text{V})^2} + \sqrt{\left(\frac{118\text{VAr}}{297\mu\text{F}\cdot(400{,}2\text{V})^2}\right)^2 + \frac{4}{33{,}4\text{mH}\cdot 297\mu\text{F}}}\right] = 50{,}7Hz \quad (81)$$

$$\omega' = \frac{1}{4\pi}\left[\frac{-109\text{VAr}}{297\mu\text{F}\cdot(404{,}7\text{V})^2} + \sqrt{\left(\frac{-109\text{VAr}}{297\mu\text{F}\cdot(404{,}7\text{V})^2}\right)^2 + \frac{4}{34{,}0\text{mH}\cdot 297\mu\text{F}}}\right] = 49{,}9Hz \quad (82)$$

In (81) the positive sign for reactive power indicates inductive power fed from the grid in prior to islanding. Negative sign in (82) indicates capacitive reactive power fed to the grid in prior to islanding. Values for reactive power are averages of measured reactive powers at PCC during 1s before islanding and voltages are averages of all three phases after islanding. There is a 0,3Hz offset in the results of (81) and (82) because of the initial resonant frequency of the islanding load is 50,3Hz rather than 50Hz. This offset can be subtracted from the results because the AFE is compensating the initial offset in LC resonance yielding to calculatory values of 50,4Hz and 49,6Hz. Values do not match the measured values exactly. It is noted that grid frequency is off of 50Hz at 49,92-49,94Hz during these tests but it seems that AFE has a tendency to keep the frequency closer to nominal than would be expected by calculations.

In figures 4.10 and 4.11, islanding without islanding detection and load inductance diverged by +/-5% is presented. Observations are similar to those with inductance diverged by +/-1% but transients are bigger and steady-state frequency is shifted further away from nominal.

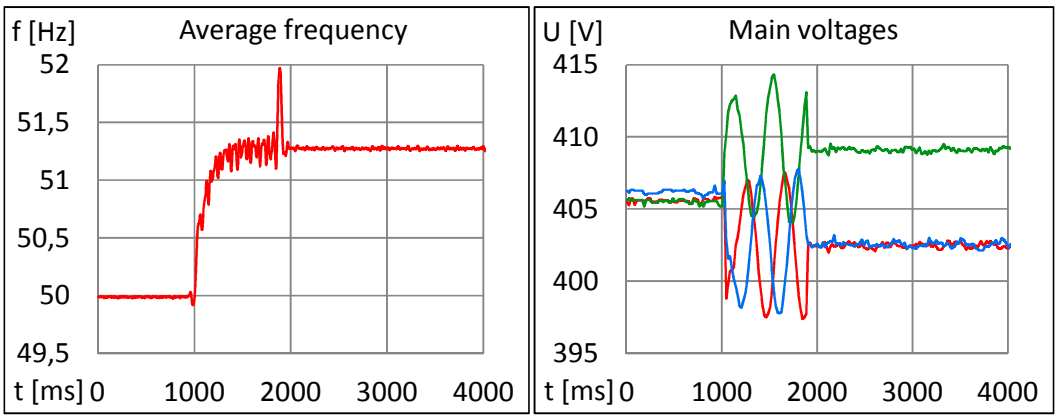

Figure 4.10. *Average system frequency and main voltages of the test setup in islanding situation without anti-islanding functionality and islanding load of 32,0mH. Red color indicates frequency and L1-to-L2 voltage, green indicates L2-to-L3 voltage and blue indicates L3-to-L1 voltage.*

Settings of the converter under testing are not changed from the initial values, i.e. it is producing same combination of active – and reactive power despite the changes in load inductance. In figure 4.10 with load inductance of 32,0mH the steady state frequency within islanded system is 51,3Hz and steady state voltages remain within acceptable range. In prior to islanding 652VAr of inductive reactive power is fed from the grid to the setup. Calculatory value for steady state frequency, calculated similarly to that in (81) and (82), is 52,7Hz which is 1,4Hz greater than measured frequency. In figure 4.11 with inductance of 35,4mH and 670VAr of capacitive reactive power fed from the setup to grid the steady state frequency of the islanded setup is 48,8Hz. Calculatory value for islanded frequency in this situation is 48,0Hz.

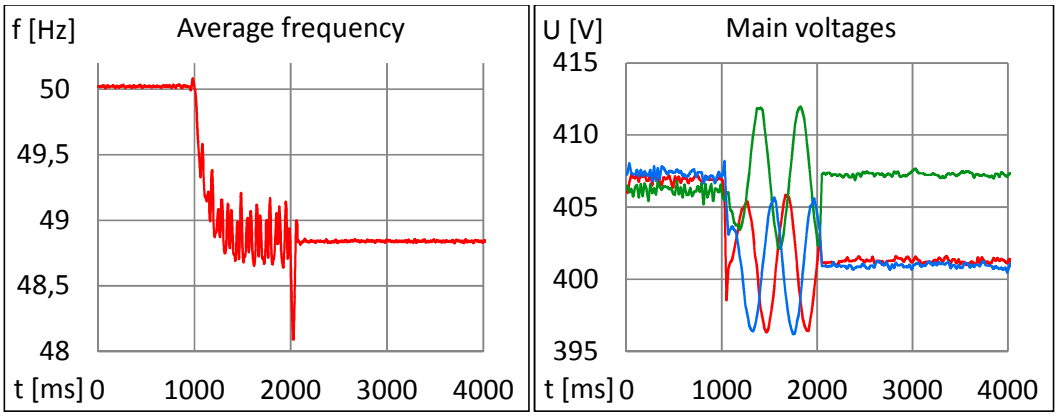

Figure 4.11. *Average system frequency and main voltages of the test setup in islanding situation without anti-islanding functionality and load inductance of 35,4mH. Red color indicates frequency and L1-to-L2 voltage, green indicates L2-to-L3 voltage and blue indicates L3-to-L1 voltage.*

These results suggest again that the setup has a tendency to maintain its frequency closer to nominal than would be expected by calculations yielding to more difficult conditions for islanding detection for e.g. protection relays. Voltage levels with these load inductances remain close to nominal but settling times for voltages are increasing with the increase of reactive power mismatch. This is mostly due to phase shift during islanding inherent from the change in frequency.

It can be concluded that without anti-islanding functionality and with PQ-balances according to [17], unintentional islanding is a high probability event. Islanding cannot be detected if thresholds for over and under frequency are +/-2,5Hz. It is evident that the steady-state frequency within the island is proportional to reactive power balance. When the active power consumption and production within the island is matched the voltage remains at its pre-islanding value. Small variations in voltage level are inherent from offsets in active power matching. Offsets occur because of small variations in grid voltage and drifting of the operation point because of e.g. heating of the resistances and other components of the setup. The asymmetry in voltages is inherent from asymmetry of the load resistances.

4.6 Testing of anti-islanding functionality

Anti-islanding functionality is tested with matched active – and reactive powers, reactive power diverged with load inductance tapping within a range of +/-2% in 1% steps and with decreased active power production. Similarly to chapter 4.5 islanding is realized with breaker BR1 in appendix 1 and settings for converter under testing are those found in chapter 4.4 and kept constant during the procedure.

4.6.1 Matched PQ-balance

In figure 4.12 islanding with anti-islanding functionality and matched PQ-balance is presented. Islanding happens at 1000ms.

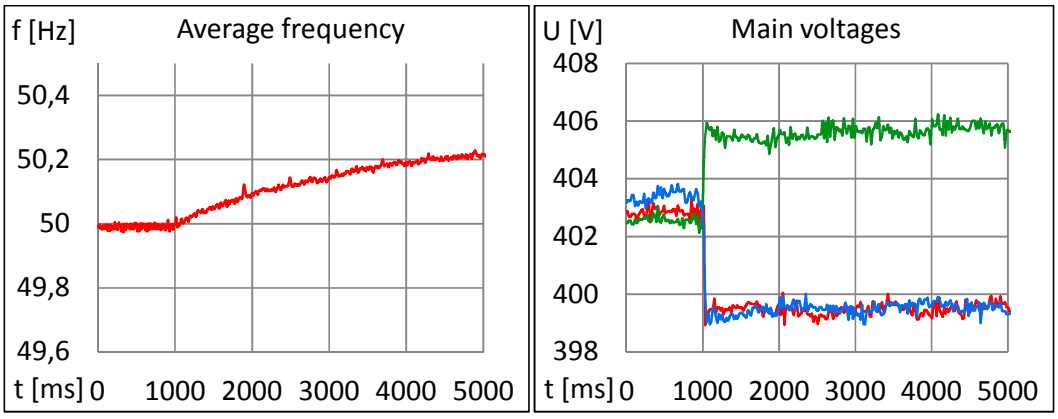

Figure 4.12. *Average system frequency and main voltages of the test setup in islanding situation with anti-islanding functionality and matched PQ balance. Red color indicates frequency and L1-to-L2 voltage, green indicates L2-to-L3 voltage and blue indicates L3-to-L1 voltage.*

Before the islanding in figure 4.12 there is 60W active power and 60VAr capacitive reactive power fed from the grid to the setup. In figure 4.13 the situation is presented with AFEs calculated frequency and reactive current over 50 seconds into islanding. It is seen from figures 4.12 and 4.13 that anti-islanding function fails to force the frequency of the system out of permissible range for operation. Operation of the anti-islanding controller can be seen in figure 4.13 where islanding happens at the moment of 5s and reactive current starts drifting as a function of frequency error. The rate of change in frequency is rather slow and does not reach 52,5Hz at any point. After the initial, faster change, the frequency starts slowly drifting back towards 50Hz. The operation of the anti-islanding controller could be also explained so that the frequency of voltage of the islanded system starts following the frequency of the inverter current. In this case the current becomes more capacitive, i.e. lags the voltage less as it is initially inductive, and system voltage frequency follows the current. In this case the positive feedback is not enough to force the frequency out of frequency window. Main voltages behavior is similar to that without anti-islanding functionality and mainly affected by the active power balance.

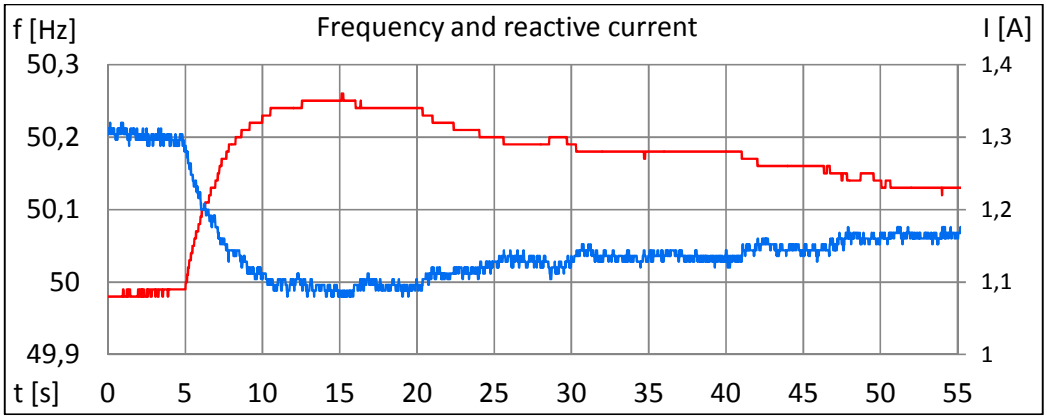

Figure 4.13. *Calculated system frequency and reactive current of the AFE with anti-islanding functionality and matched PQ balance. Red color indicates frequency and blue indicates reactive current.*

4.6.2 Diverged load inductance

Islanding with anti-islanding functionality and load inductance diverged by +/-1% to 33,4mH and 34mH is presented in figures 4.14 and 4.15, respectively. In the situation of figure 4.14 the reactive power unbalance in prior to islanding is approximately 100VArs inductive power fed from the grid to the setup. This is enough to force the frequency out of the frequency window but for the limits of +/-2,5Hz the requirement of tripping in two seconds is not met.

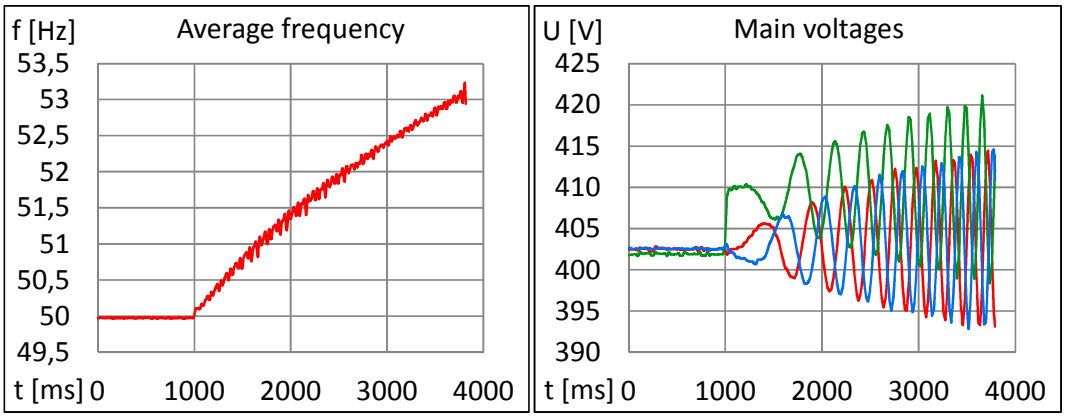

Figure 4.14. *Average system frequency and main voltages of the test setup in islanding situation with anti-islanding functionality and load inductance of 33,4mH. Red color indicates frequency and L1-to-L2 voltage, green indicates L2-to-L3 voltage and blue indicates L3-to-L1 voltage.*

In the situation of figure 4.15 with 34,0mH load inductance the reactive power mis-match before islanding is approximately 170Vars capacitive power fed from the setup to the grid. The threshold of 47,5Hz is reached in about 2,3 seconds by a spike occurring at the settling of voltages. If there was enough filtering or delay in frequency monitoring this spike wouldn't trigger the protection and the threshold would be reached at 3,2s.

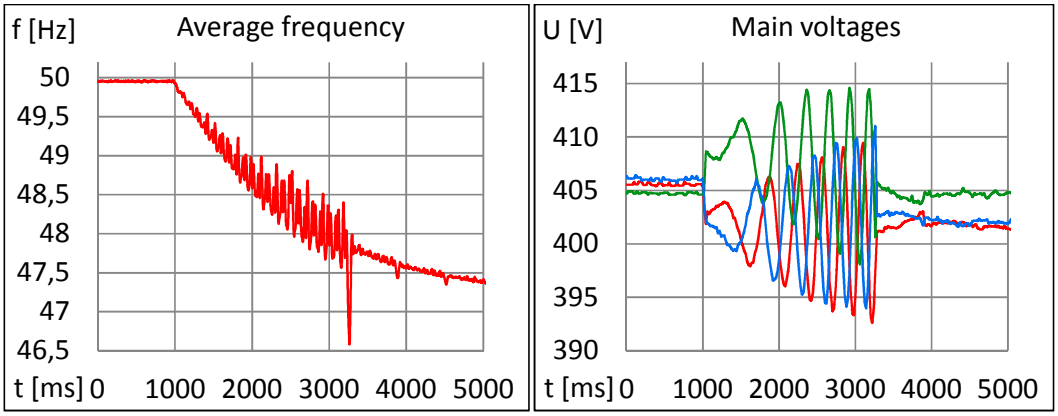

Figure 4.15. *Average system frequency and main voltages of the test in islanding situation with anti-islanding functionality and load inductance of 34,0mH. Red color indicates frequency and L1-to-L2 voltage, green indicates L2-to-L3 voltage and blue indicates L3-to-L1 voltage.*

Settling of the voltages is a point where the rate of change in frequency becomes small enough for the AFE synchronizer to keep inverter terminal voltages synchronized with the frequency stated by the load. The sign of reactive power fed by the AFE depends on the initial change in frequency. If the change initially is negative, as in figure 4.15 where system reactive power balance is at less than 50Hz, the additive reactive current is also inductive, i.e. it will cause the inverter current to lag more or gain less in relation to voltage and thereby decrease also the frequency of voltage, and vice versa. In both cases with 1% diverged inductance voltages are subject to oscillations but the RMS values still remain inside permissible range.

In figure 4.16 a) and b) the behavior of the system with load inductance values 33,0mH and 34,4mH, i.e. +/-2% is presented. With 33mH approximately 220VArs of inductive reactive power is fed from the grid to the system and with 34,4mH approximately 300VArs of capacitive reactive power is fed to the grid. In both cases the frequency drifts out of the frequency window in about 800ms.

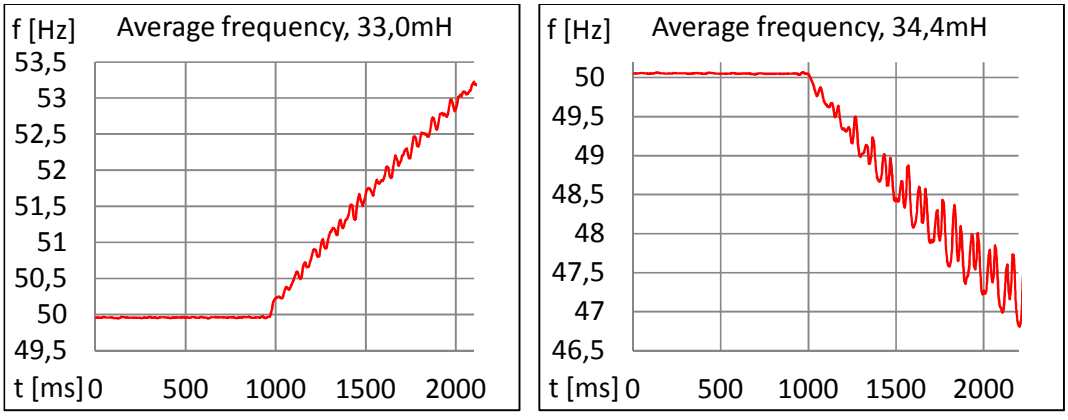

a) **b)**

Figure 4.16. *Average system frequencies of the test setup in islanding situation with anti-islanding functionality and load inductances of 33,0mH and 34,4mH.*

With higher than +/-2% divergence in load inductances the tripping time keeps shortening. Voltage behavior in all cases is similar to that with load inductances 33,4mH and 34,0mH. The amplitude of oscillations keeps increasing with the increase of reactive balance divergence but in all cases voltage remains within acceptable range.

4.6.3 Active power imbalance

In [17] testing also with different active power levels is required. In figure 4.17 an islanding situation with matched reactive power and 4,4kW active power production is presented. 4,4kW is 67% of the matched production of 6,6kW in previous tests and 53% of the nominal power of 8,28kW of the inverter under testing.

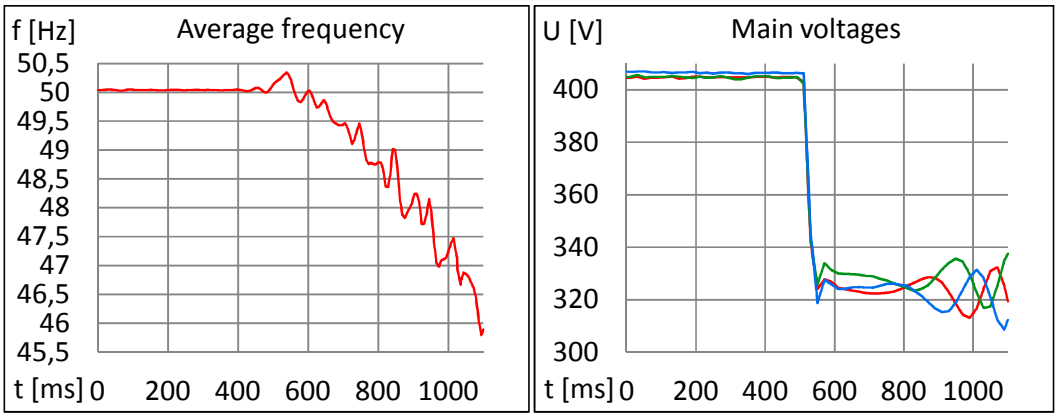

Figure 4.17. *Average system frequency and main voltages of the test setup in islading situation with reduced active power production and matched reactive power. Red color indicates frequency and L1-to-L2 voltage, green indicates L2-to-L3 voltage and blue indicates L3-to-L1 voltage.*

In figure 4.18 the behavior of active – and reactive currents during islanding is presented. At the moment of islanding AFE is supplying 6,3A active current. Islanding results in dropping of the main voltages to a level of 325V. Calculatory value for islanded system voltage in this case is 317V. Dropping of voltage level results in reactive power imbalance which starts to affect the system frequency and this change is amplified by the anti-islanding controller. It is seen that the dropping of voltages results in active current increasing to a level which is sufficient to keep DC voltage in control. Thus, active power balance is maintained when voltage settles to a level at which resistances consume the power produced by AFE. Also reactive current level is affected by the voltage drop. Reactive current is affected because of the AFE's filter compensation function which takes into account changes in active current. Changes in active current affect the reactive power of AFE's filtering. Anti-islanding controller does not react to a small rise in frequency immediately after islanding at 200ms in figure 4.18 but starts to amplify the frequency divergence after that.

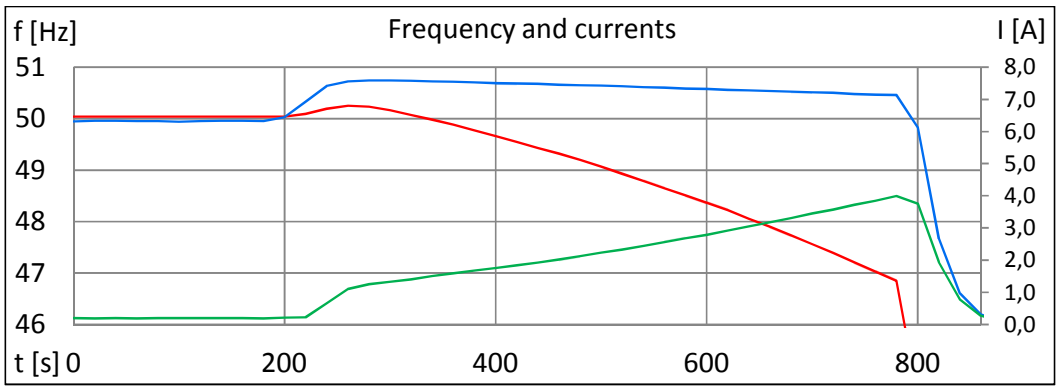

Figure 4.18. *System frequency and currents of the test setup in islanding situation with reduced active power production and matched reactive power. Red color indicates frequency, green reactive – and blue active current.*

Reactive power balance within the setup is not maintained despite the facts that the LC loads resonance is not affected by voltage level and AFE takes into account also changed reactive power of its filter inductance. This imbalance after islanding have to be explained by the fact that AFE does not take into account actual voltage level in filter compensation which affects the filter capacitance's reactive power and reactive unidealities within the setup. Although system voltages drop outside acceptable range almost immediately this could be interpreted as a grid fault and thus would not cause tripping of the AFE if FRT functionality is active. With FRT functionality there will be a delay in islanding detection which is dependent on voltage level and FRT voltage characteristics. After the islanding at 500ms in figure 4.17 the frequency drifts out of the frequency window of +/-2,5Hz in 450ms.

4.6.4 Effects of AFE settings

In the tested AFE there is many parameters which are designed for other features than anti-islanding but affect also the performance of anti-islanding function. Also, there is available a gain parameter for the anti-islanding controller positive feedback gain. Gain parameter's default setting is 50% which is the value all presented tests are done with. It should be noted that finding the appropriate value for each application might be difficult and should be done case-by-case. Also, it is possible that suitable setting for gain could change after commissioning of the system. It is possible to communicate the setting from upper level control system if one exists but different scenarios for e.g. grid configuration could be hard to determine theoretically before they can be tested. Effects of different gain settings were tested briefly and results yield that a higher gain results in shorter tripping times and vice versa. Gain parameter setting will also have an effect on the overall performance of the AFE as possible nuisance tripping and undesired reactive power injections in case of frequency variations in the grid.

Reactive power production of the AFE can also be affected by other features, e.g. voltage support function. Voltage level based reactive current injection was also tested and it is possible that this function will decrease the probability of successful islanding

prevention. If the initial change in voltages after islanding is such that the resulting reference for reactive current is opposite to that of anti-islanding controller it is evident that the performance of islanding prevention is affected negatively. A logic in which these functions wouldn't disturb each other could be e.g. such that voltage support control works slower than anti-islanding. However, in this solution anti-islanding would be disabled from applications in which the grid voltage level is pushed down to have marginal in DC voltage. One possibility would be for the anti-islanding controller to have priority over voltage support when islanding is suspected because of e.g. change in system frequency.

It is possible that AFE's current limit affects islanding detection. If there is enough active power production it is possible that the reactive current produced by anti-islanding controller couldn't force the frequency outside the frequency window when total current is limited by current limit. However, usually AFE is capable of producing significantly more than its nominal current in short term. Setting of current limit is something that has to be taken into account when making islanding considerations. Also, it would be possible to increase the probability of islanding prevention by having priority of reactive current over active current when islanding is suspected. Especially in a case of megawatt class inverters and wind – or solar parks, but also smaller scale units it is highly dependent on the grid configuration of the islanded power system how much a single inverter is capable of deviating the frequency even with maximum current.

Frequency range in which a modern inverter unit is able to operate is very large. From the control point of view it is not obligatory to stop modulation or trip the unit in case of over – or under frequency. Therefore, with an anti-islanding function operating on AFE output frequency it is necessary to define the limits for permissible frequency range case-by-case and in collaboration with turbine manufacturer.

5 CONCLUSIONS

The purpose of this thesis was to study islanding phenomenon and islanding detection methods from perspective of a full power converter as well as design and build a test facility for islanding studies. Effects of islanding and different islanding detection methods were studied as a literature survey and test setup was utilized for testing of an inverter in islanding situation. Significant amount of time was used for planning and building of the test setup.

Many of the available islanding detection methods are not suitable for implementation into a DG unit because they are complicated and require large amount computing capacity or extremely accurate measuring equipment. In the future it is likely that hybrid methods gain more interest since requirements for power quality exclude many active methods and passive methods are excluded by their ineffectiveness. Some of the presented islanding detection methods could be implementable into a DG inverter grid interface and operational as they are but also modifications and applicability into different environments has to be thought through. Most promising ones presented in this thesis are adaptive logic phase shift from active methods and hybrid method combining covariance of voltage and current periods and adaptive reactive power shift. Also, possibility of combinations like covariance of voltage and current periods or rate of change of frequency over power with ALPS or AFD could be effective in islanding detection without too much affecting power quality and other functionality of the inverter.

Islanding test setup was built in accordance to IEEE standardization. The core component of the test setup is a parallel RLC load which is sized to resonate at grid frequency. Grid frequency resonant load is to increase the probability of the islanded system to maintain grid frequency close to nominal. With a 4Q drive which is able to supply wanted active – and reactive power combination limited mainly by current capabilities it is the overall reactive power balance rather than the capacitive-inductive load balance of the islanded system which defines the steady state frequency of the islanded system and thus, probability of unintentional islanding. If the islanded section contains also synchronous machines equipped with voltage and frequency control, the behavior of the system becomes different and frequency is no longer dependent only on the reactive power balance. Also, within an islanded system containing only power electronics controlled distributed generation, the voltages of the system are proportional to active power balance within that system.

With tested grid interface inverter and without islanding prevention function islanding proved to be a relatively high probability event. In this case unintentional islanding happens if reactive – and active power balances are within a range which yields to fre-

quency and voltages of the islanded system remaining inside acceptable values. From inverter control point of view the range for frequency in which it is possible to operate is very wide and limits for frequency window have to be set in accordance to grid regulations. Reactive – or active power mismatch required for prevention of unintentional islanding depends on the configuration of the islanded grid section but also on applied grid code, i.e. frequency and voltage operation ranges.

With used anti-islanding method which is based on reactive current injection on basis of frequency error, it is characteristic that with perfect matching of reactive – and active power balance islanding cannot be prevented because the frequency error does not occur. Load inductance divergence of +/-1% resulted in reactive power imbalance of 100VArs inductive and 170VARs capacitive within the island. In these situations islanding was prevented but not in two seconds required by standardization. With greater reactive power imbalances the islanding was prevented in less than two seconds. Based on these values it can be approximated that reactive power imbalance needed for successful islanding prevention in this case is about 200VArs which is 1,3% of the reactive power produced and consumed by the LC load. This can be referred to as NDZ of the tested islanding detection method.

Voltage levels are not significantly affected by reactive power imbalance within a power system containing only non-synchronous DG. However, voltages are subject to change because of active power imbalance and dropping of voltages also affects the reactive power balance within the islanded system. In worst case it could equalize inductive and capacitive power productions within the island resulting in failure to prevent islanding. As the current trend with regulations for distributed generation is that a DG unit has to survive within a wide voltage range and also from grid faults even with zero remaining voltage it is evident that voltage level based islanding detection is very difficult.

Continuation of islanding studies should be done with respect to different kinds of configurations of the islanded grid section, i.e. a system containing other inverters and/or synchronous machines. The possible use of currently available islanding prevention method should be done with respect to other features of the grid inverter to not interfere normal operation. It should be also examined how the anti-islanding function will affect normal operation and e.g. FRT functionality of a mega-watt class converter system. The next step from islanding detection is the operational island. With current products there is a possibility allowing inverter operation as a voltage source controlling its voltage and frequency on basis of reactive power – voltage and active power – frequency droops. However, the transition from grid connected operation to island mode operation is not possible with modulating inverter. This limitation rules out the possibility of direct continuation of operation in an island and changing of control mode has to be done manually or in the upper level of grid automation.

REFERENCES

[1] Short, T.A. Electric Power Distribution Handbook. New York, NY, USA 2003, CRC Press. 784 p.

[2] Antikainen, J., Repo, S., Verho, P., Järventausta, P. Possibilities to Improve Reliability of Distribution Network by Intended Island Operation. International Journal of Innovations in Energy Systems and Power 4(2009)1, pp. 22-28.

[3] Barker, P. P., de Mello, R. W. Determining the Impact of Distributed Generation on Power Systems: Part 1 – Radial Distribution Systems. Power Engineering Society Summer Meeting, Seattle, WA, USA, 16th – 20th June 2000. New York, USA 2000, IEEE. Pp. 1645-1656.

[4] Barker, P. Overvoltage Considerations in Applying Distributed Resources on Power Systems. Power Engineering Society Summer Meeting, Chicago, IL, USA, 25th July 2002. New York, USA 2002, IEEE. Pp. 109-114.

[5] Larsson, Å. Flicker Emission of Wind Turbines During Continuous Operation. IEEE Transactions on energy conversion 17(2002)1, pp. 114-118.

[6] Mehrizi-Sani, A., Filizadeh, S., Wilson, P.L., Harmonic and Loss Analysis of Space-Vector Modulated Converters. International Conference on Power Systems Transients, Lyon, France, 4th – 7th June 2007. IPST 2007. 6 P.

[7] Sähköenergialiitto ry SENER, Pienvoimaloiden liittäminen jakeluverkkoon, Publication series 3/01, Helsinki 2001, 25 p.

[8] Walling, R.A. Distributed Generation Islanding – Implications on Power System Dynamic Performance. 2002 IEEE Power Engineering Society Summer Meeting 2(2002), pp. 92-96.

[9] Peças Lopes, J. A., Moreira, C. L., Madureira, A. G. Defining Control Strategies for MicroGrids Islanded Operation. IEEE Transactions on power systems 21(2006)2, pp. 916-924.

[10] Skvarenina, T. L. The Power Electronics Handbook. Schenectady, New York, NY, USA 2002, CRC Press. 664 p.

[11] Neacsu, D. O. Power-Switching Converters Medium and High Power. New York, NY, USA 2006, CRC Press. 384 p.

[12] Firmware interface active front-end. 17.1.2007. Vacon Oyj. Confidential report. 14 p.

[13] Hsieh, G.-C., Hung, J. C. Phase-Locked Loop Techniques – A Survey. IEEE Transactions on industrial electronics 43(1996)6, pp. 609-615.

[14] Barsali, S., Ceraolo, M., Pelacchi, P., Poli, D. Control techniques of Dispersed Generators to improve the continuity of electricity suppply. Power Engineering Society Winter Meeting 2(2002), pp. 789-794.

[15] Mahat, P., Chen, Z., Bak-Jensen, B. Review of Islanding Detection Methods for Distributed Generation. Electric Utility Deregulation and Restructuring and Power Technologies, Nanjing, China, 6th – 9th April 2008. Pp. 2743-2748.

[16] De Mango, F., Liserre, M., Aquila, A.D., Pigazo, A. Overview of Anti-Islanding Algorithms for PV Systems. Part 1: Passive Methods. Power Electronics and Motion Control Conference, Portorož, Slovenia 30th August – 1st September 2006. New York, USA 2006, IEEE. Pp. 1878-1883.

[17] IEEE 1547.1. IEEE Standard Conformance Test Procedures for Equipment Interconnecting Distributed Resources with Electric Power Systems. New York, USA 2005, IEEE. 44 p.

[18] IEEE 929-2000. Recommended practice for Utility Interface of Photovoltaic (PV) Systems. New York, USA 2000, IEEE, 10p.

[19] Kunte, R. S., Gao, W. Comparison and Review of Islanding Detection Techniques for Distributed Energy Resources. 40th North American Power Symposium, Galgary, Canada, 28th -30th September 2008. New York, USA, 2008, IEEE. Pp 1-8.

[20] Ezzt, M., Marei, M. I., Abdel-Rahman, M., Mansour M. M. A Hybrid Strategy for Distributed Generators Islanding Detection. Power Engineering Society Conference and Exposition in Africa, Johannesburg, South Africa, 16th – 20th July 2007. New York, USA 2007, IEEE. Pp. 1-7.

[21] Bright, C. G. COROCOF: Comparison of rate of change of frequency protection. A solution to the detection of loss of mains. 7th International Conference on Developments in Power System Protection, Amsterdam, Netherlands, 9th – 12th April 2001. Pp. 70-73.

[22] Pai F-S., Hung S-J. A Detection Algorithm for Islanding-Prevention of Dispersed Consumer-Owned Storage and Generating Units. IEEE Transactions on energy conversion 16(2001)4, pp. 346-351.

[23] De Mango, F., Liserre, M., Aquila, A.D., Pigazo, A. Overview of Anti-Islanding Algorithms for PV Systems. Part 2: Active Methods. Power Electronics and Motion Control Conference, Portorož, Slovenia 30th August – 1st September 2006. New York, USA 2006, IEEE. Pp. 1884-1889.

[24] Asiminoaei, L., Teoderescu, R., Blaabjerg, F., Borup, F. A New Method of On-line Grid Impedance Estimation for PV Inverter. Nineteenth Annual IEEE Applied Power Electronics Conference and Exposition, 3(2007), pp. 1527-1533.

[25] Ciobotaru, M., Teoderescu, R., Blaabjerg, F. On-line grid impedance estimation based on harmonic injection for grid-connected PV inverter. International symposium on Industrial Electronics, Vigo, Spain 4th -7th June 2007. New York, USA 2007, IEEE. Pp. 2437-2442.

[26] Stevens, J., Bonn, R., Ginn, J., Gonzales, S. Development and Testing of an Approach to Anti-Islanding in Utility-Interconnected Photovoltaic Systems. Boulder, USA, 2000, Sandia National Laboratories, Photovoltaic System Applications Department. 58 p.

[27] Zhu, X., Shen, G., Xu, D. Evaulation of AFD Islanding Detection Based on NDZs Described in Power Mismatch Space. Energy Conversion Congress and Exposition, San Jose, USA 20th – 24th September 2009. New York, USA 2009, IEEE. Pp. 2733-2739.

[28] Jung, Y., Choi, J., Yu, G., Yu, P., So., J., Choi, J. A Novel Active Frequency Drift Method of Islanding Prevention for the grid-connected Photovoltaic Inverter. IEEE 36th Power Electronics Specialists Conference, Recife, Brazil, 12th – 16th June 2005. New York, USA 2005, IEEE. Pp. 1915-1921.

[29] IEEE 1547-2003. IEEE Standard for Interconnecting Distributed Resources with Electric Power Systems. New York, USA 2003, IEEE. 15p.

[30] Ropp, M.E., Begovic, M., Rohatgi, A. Analysis and performance assessment of the active frequency drift method of islanding prevention. IEEE Transactions on Energy Conversion 14(1999)3, pp. 810-816.

[31] Smith, G.A., Onions, P.A., Infield, D.G. Predicting islanding operation of grid connected PV inverters. IEEE Proceedings – Electric Power Applications 147(2000)1, pp. 1-6.

[32] Hung, G.-K., Chang, C.-C., Chen, C.-L. Automatic Phase-Shift Method for Islanding Detection of Grid-Connected Photovoltaic Inverters. IEEE Transactions on energy conversion, 18(2003)1, pp. 169-173.

[33] Liu, F., Kang, Y., Zhang, Y., Duan, S., Lin, X. Improved SMS islanding detection method for grid-connected converters. IET Renewable Power Generation 4(2010)1, pp. 36-42.

[34] Yin, J., Chang, L., Diduch, C. A New Adaptive Logic Phase-Shift Algorithm For Anti-Islanding Protections In Inverter-Based DG System. IEEE 36th Power Electronics Specialists Conference, Recife, Brazil, 12th – 16th June 2005. New York, USA 2005, IEEE. Pp. 2482-2486.

[35] Menon, V., Hashem Nehrir, M. A Hybrid Islanding Detection Technique Using Voltage Unbalance and Frequency Set Point. IEEE Transactions on power systems, 22(2007)1, pp. 442-448.

[36] Yin, J., Chang, L., Diduch, C. A New Hybrid Anti-Islanding Algorithm in Grid Connected Three-Phase Inverter System. 37th IEEE Power Electronics Specialists Conference, JeJu, South-Korea, 18th -22nd June 2006. New York, USA 2006, IEEE. Pp. 1-7.

[37] Cobreces, S., Bueno, E. J., Pizarro, D., Rodriguez, F. J., Huerta, F. Grid Impedance Monitoring System for Distributed Power Generation Electronic Interface. IEEE Transactions on instrumentation and measurement 58(2009)9, pp. 3112-3121.

[38] Cobreces, S., Huerta, F., Pizarro, D., Rodriguez, F. J., Bueno E. J. Three-phase power system parametric identification based on compex-space recursive least squares. IEEE International Symposium on Intelligent Signal Processing, Alcala de Henares, Spain 3rd – 5th October 2007. New York, USA, 2007 IEEE. Pp. 1-6.

[39] China Electric Power Research Insititute. Chinese Danish Wind Energy Development Programme Technical Report [WWW]. [Referred 14.12.2011] Available: http://www.dwed.org.cn/uploadfiles/20109915445/wed-qr-c01-e-05.pdf

[40] Vainikka, J-P. Hajautetun tuotannon verkkoon liittäminen – verkkokoodit ja käytännön toimet. Diplomityö, Lappeenrannan Teknillinen Yliopisto, 2011.

[41] Woyte, A., Belmans, R., Nijs, J. Testing the Islanding Protection Function of Photovoltaic Inverters. IEEE Transactions on Energy Conversion 18(2003)1, pp. 157-162.

[42] Dorf, C. R. The Electrical Engineering Handbook, Second Edition. Boca Raton, Florida, USA 2000, CRC Press. 2752 p.

APPENDIX 1

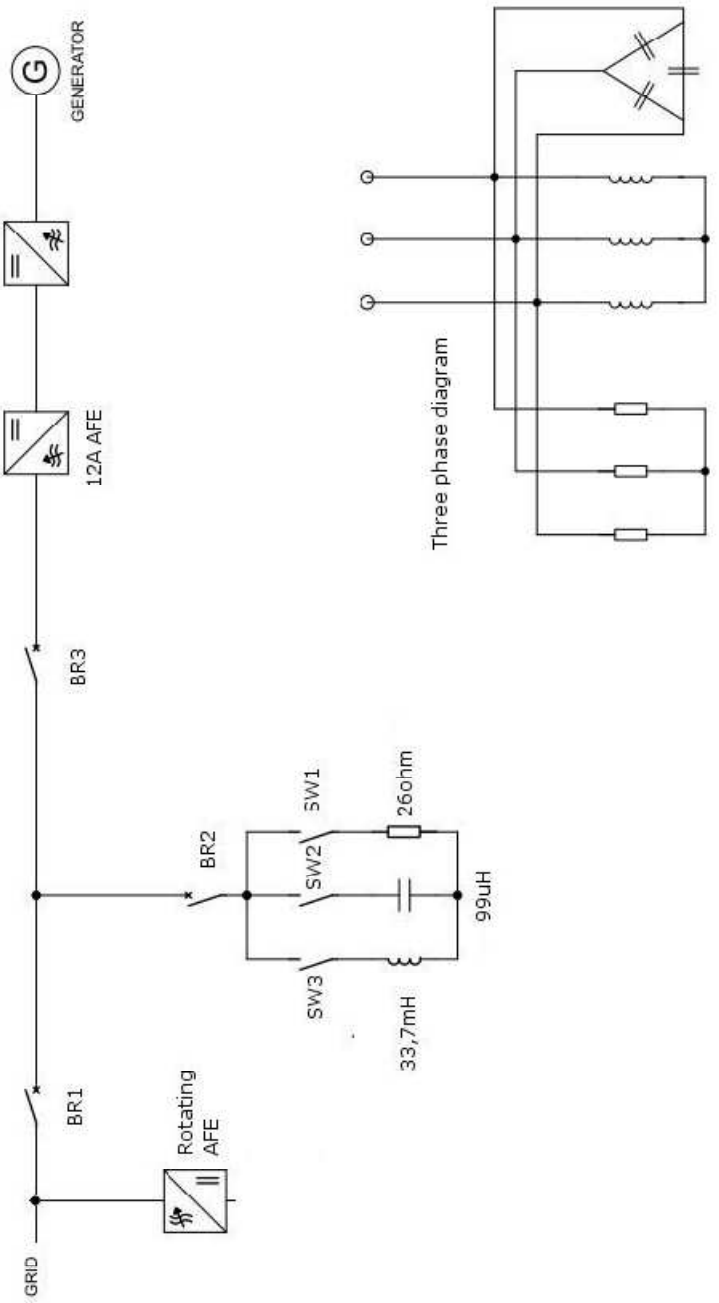
GENERATOR
12A AFE
BR3
BR2
SW1
26ohm
SW2
99uH
SW3
33,7mH
BR1
Rotating AFE
GRID
Three phase diagram